

M.THESIS

19

EVALUATION OF THE EFFECTS OF THE PARAMETER VARIATIONS ON THE  
PERFORMANCE OF THE FEED DRIVE SYSTEMS FOR N.C. MACHINE TOOLS

A MASTER'S THESIS

in

Mechanical Engineering

Middle East Technical University

043552

By

İbrahim H. GÜZELBEY


March 1985

Approval of the Graduate School of Natural and Applied Sciences.

  
Prof. Dr. Bilgin KAFTANOĞLU

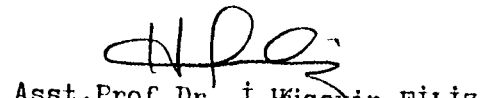
Director

I certify that this thesis satisfies all the requirements as a thesis for the degree of Master of Science in Mechanical Engineering Department.

  
Prof. Dr. Alp ESİN

Chairman of the Department

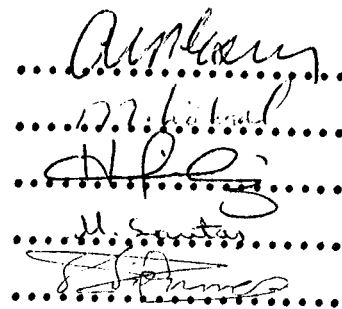
We certify that we have read this thesis and that in our opinion it is fully adequate, in scope and quality, as a thesis for the degree of Master of Science in Mechanical Engineering Department.

  
Asst. Prof. Dr. İ. Hüseyin FİLİZ

Supervisor

Examining Committee in Charge :

Prof. Dr. Alp ESİN (Chairman)  
Assoc. Prof. Dr. Muhammed KÖKSAL  
Asst. Prof. Dr. İ. Hüseyin FİLİZ  
Asst. Prof. Dr. Müzeyyen SARITAŞ  
Asst. Prof. Dr. Ali İhsan SÖNMEZ



## ABSTRACT

EVALUATION OF THE EFFECTS OF THE PARAMETER VARIATIONS ON THE PERFORMANCE OF THE FEED DRIVE SYSTEMS FOR N.C. MACHINE TOOLS

GÜZELBEY, İbrahim Halil

M.S. in Mechanical Engineering

Supervisor : Asst.Prof.Dr.İ.Hüseyin FİLİZ

March 1985, 86 Pages

This thesis is a theoretical investigation of the effect of the parameter variation on the dynamic performance of nc machine tools feed drives by using analog simulation method.

In this study, lumped parameter approach is used to model the system. Friction is included in the model as a non - linear parameter. The control system of the feed drive is considered as a position and velocity feedback loops without compensation. System is examined under these conditions.

Two inertia model is considered to be enough to analyse the feed drive system. Analog simulation is illustrated by an example whose parameters are chosen from a real machine tool.

Key Words : analog simulation, feed drive system, dynamic performance.

## ÖZET

NÜMERİK KONTROLLU TAKIM TEZGAHLARININ KIZAK TAHRİK SİSTEMLERİNİN  
PERFORMANSI ÜZERİNDE PARAMETRELERİN DEĞİŞİM ETKİSİNİN İNCELENMESİ

GÜZELBEY, İbrahim Halil

Yüksek Lisans Tezi, Makina Mühendisliği Bölümü

Tez Yöneticisi : Yard.Doç.Dr.İ.Hüseyin FİLİZ

Mart 1985, 86 Sayfa

Bu tez, örneksel benzeşim yöntemiyle sayısal kontrollu takım tezgahlarının kızak tahrik sisteminin dinamik performansı üzerinde, parametre değişimlerinin teorik incelenmesidir.

Bu çalışmada, sistemi modellemek için kümelenmiş kitle yaklaşımı kullanılmıştır. Sürtünme, linear olmayan parametre olarak modele dahil edilmiştir. Kızak tahrik mekanizmasının kontrol sistemi, kompenzasyonsuz konum ve hız çevrimlerinden oluştuğu kabul edilmiştir. Sistem bu şartlar çerçevesinde incelenmiştir.

Kızak tahrik sistemini analiz etmek için ikili kitle modelinin yeterli olduğu kabul edilmiştir. Örneksel benzeşim, gerçek bir takım tezgahından seçilen parametreler kullanılarak bir örnekle gösterilmiştir.

Anahtar Kelimeler : örneksel benzeşim, kızak tahrik sistemi, dinamik performans.

## ACKNOWLEDGEMENTS

I would like to express my gratitude to Asst.Prof.Dr.İ.Hüseyin Filiz for his kind supervison, encouragement and valuable comments.

I am grateful too, to Prof.Dr.Alp Esin, Head of the Department of Mechanical Engineering for his helps in various subjects.

I feel thankful also to Asst.Prof.Dr.Süleyman Sarıtaş, Asst. Prof.Dr. Sedat Bayseç and Research Assistant Gökhan Dai from Mechanical Engineering Department for their kind encouragements.

Lastly, I thank to Tülây Ardiç for her correct typing, to Ayşegül Dalbudak for tracing the figures and to Emel Bahçeci for taking photographes.

## TABLE OF CONTENTS

	Page
ABSTRACT .....	iii
ÖZET .....	iv
ACKNOWLEDGEMENT .....	v
LIST OF TABLES .....	viii
LIST OF FIGURES .....	iv
NOMENCLATURE .....	xii
1. INTRODUCTION .....	1
2. LITERATURE SURVEY .....	3
2.1. Introduction .....	3
2.2. Feed Drive Modelling .....	3
2.3. Analog Simulation .....	5
3. FEED DRIVE MODELLING .....	8
3.1. Introduction .....	8
3.2. The General View on Modelling and Feed Drive .....	8
3.3. Modelling of Feed Drive and Deriving the Model Equations .....	11
3.3.1. DC Motor Model .....	11
3.3.2. Coupling Model .....	14
3.3.3. Leadscrew Assembly Model .....	14
3.3.3.1. Torsional Model.....	15
3.3.3.2. Axial Model .....	18
3.3.4. Friction Model .....	21
3.3.5. Backlash and its Model.....	26
3.4. Model Equations .....	27
4. ANALOG SIMULATION .....	34
4.1. Introduction .....	34
4.2. Analog Simulation .....	34
4.3. Analog Computer .....	35

## LIST OF FIGURES

Figure	Page
3.1. General Arrangement of a Numerical Controlled Feed Drive Axis. ....	10
3.2. Equivalent Circuit for D.C. Motor .....	12
3.3. Speed - Torque and Current - Torque Curve of PM DC Motor.	13
3.4. DC Motor Models .....	13
3.5. A Coupling and its Model .....	14
3.6. Double Ended Leadscrew Assembly Configuration and its Model .....	16
3.7. Single Ended Leadscrew Assembly Configuration and its Model .....	16
3.8. Axial Model of Double Ended Leadscrew Assembly .....	19
3.9. Axial Model of Single Ended Leadscrew Assembly .....	20
3.10. Torsional Equivalent of Axial Models .....	21
3.11. Combined Model of Leadscrew Assemblies .....	22
3.12. Combined Non - linear Model of Leadscrew Assembly .....	23
3.13. Linear Model of Feed Drive .....	24
3.14. Non - linear Models of Feed Drive .....	25
3.15. Friction Models .....	26
3.16. Backlash Representation and its Model .....	27
3.17. Normalised Block Diagram of Position Control System with Unity Feedback .....	28
3.18. Five Inertia Model of the Feed Drive .....	29
3.19. Two Inertia Model of Feed Drive .....	32
3.20. Two Inertia Non - Linear Model .....	33
4.1. An Analog Inverter .....	35
4.2. Summer .....	36

	Page
4.4. Magnitude and Time Scaling .....	37
4.4.1. Time Scaling .....	37
4.4.2. Magnitude Scaling .....	39
4.4.3. Estimation of Maximum Values .....	40
4.5. Scaled Equations and Block Diagram for the Feed Drive Model .....	45
5. EVALUATION OF DYNAMIC PERFORMANCE .....	57
5.1. Introduction .....	57
5.2. Experimental Set - up .....	57
5.3. Illustrative Example .....	59
5.3.1. Setting up the Example .....	59
5.3.2. Analog Simulation .....	61
6. DISCUSSION AND CONCLUSION .....	81
6.1. Discussion .....	81
6.2. Conclusion .....	83
6.3. Suggestions for Future Work .....	83
REFERENCES .....	84
APPENDIX .....	86



LIST OF TABLES

Table	Page
3.1. Inertia of the Five Inertia Model .....	30
3.2. Stiffness Values in the Five Inertia Model .....	31
3.3. Inertia of the Two Inertia Model .....	31
4.1. Sembolic Representation of Potentiometers For Figure 4.5.....	53
4.2. Symbolic Representation of Potentiometers for Figure 4.6.....	54
4.3. Sembolic Representation of Potentiometers For Figure 4.7.....	55
4.4. Sembolic Representation of Potentiometers For Figure 4.5.....	56
5.1. Parameter Values .....	61
5.2. Inertia of the Components .....	61
5.3. Estimated Maximum Values .....	62
5.4. Values of the Potentiometers .....	65

4.3. Integrator .....	36
4.4. Potentiometer .....	36
4.5. Analog Computer Diagram For Five Inertia Linear Model (L) ...	49
4.6. Analog Computer Diagram for Two Inertia Linear Model (L) .....	50
4.7. Analog Computer Diagram for Two Inertia Linear Model (L=0) ...	51
4.8. Analog Computer Diagram for Two Inertia Non - Linear Model (L = 0) .....	52
5.1. Experimental Set - up .....	58
5.2. Layout of Feed Drive Axes .....	60
5.3. Analog Computer Diagram for Two Inertia Linear Model .....	63
5.4. Analog Computer Diagram for Two Inertia Non - Linear Model ..	64
5.5. System Response at Original Parameter Values .....	67
5.6. Effect of $K_{eaT}$ ( $K_{eaT}^* = 4 K_{eaT}$ ) .....	68
5.7. Effect of $K_{eaT}$ ( $K_{eaT}^* = 3 K_{eaT}$ ) .....	68
5.8. Effect of $K_{eaT}$ ( $K_{eaT}^* = 2 K_{eaT}$ ) .....	69
5.9. Effect of $K_{eaT}$ ( $K_{eaT}^* = \frac{1}{2} K_{eaT}$ ) .....	69
5.10. Effect of $K_{eaT}$ ( $K_{eaT}^* = \frac{1}{3} K_{eaT}$ ) .....	70
5.11. Effect of $K_{eaT}$ ( $K_{eaT}^* = \frac{1}{4} K_{eaT}$ ) .....	70
5.12. Effect of the Equivalent Slide Inertia ( $J_2^* = 4 J_2$ ) .....	71
5.13. Effect of the Equivalent Slide Inertia ( $J_2^* = 3 J_2$ ) .....	71
5.14. Effect of the Equivalent Slide Inertia ( $J_2^* = 2 J_2$ ) .....	72
5.15. Effect of the Equivalent Slide Inertia ( $J_2^* = \frac{1}{2} J_2$ ) .....	72
5.16. Effect of the Equivalent Slide Inertia ( $J_2^* = \frac{1}{3} J_2$ ) .....	73
5.17. Effect of the Damping ( $D_{tT}^* = 4D_{tT}$ ) .....	73
5.18. Effect of the Damping ( $D_{tT}^* = 3D_{tT}$ ) .....	74
5.19. Effect of the Damping ( $D_{tT}^* = 2D_{tT}$ ) .....	74
5.20. Effect of the Damping ( $D_{tT}^* = \frac{1}{2}D_{tT}$ ) .....	75
5.21. Effect of the Damping ( $D_{tT}^* = \frac{1}{3}D_{tT}$ ) .....	75
5.22. Effect of the Loop Gains ( $K_p^* = \frac{1}{4} K_p$ and $K_v^* = 4 K_v$ ) .....	76
5.23. Effect of the Loop Gains ( $K_p^* = \frac{1}{3} K_p$ and $K_v^* = 3 K_v$ ) .....	76

5.24.Effect of the Loop Gains ( $K_p^* = \frac{1}{2} K_p$ and $K_v^* = 2 K_v$ ) .....	77
5.25.Effect of the Loop Gains ( $K_p^* = 2 K_p$ and $K_v^* = \frac{1}{2} K_v$ ) .....	77
5.26.Effect of the Loop Gains ( $K_p^* = 3 K_p$ and $K_v^* = \frac{1}{3} K_v$ ) .....	78
5.27.Effect of the Loop Gains ( $K_p^* = 4 K_p$ and $K_v^* = \frac{1}{4} K_v$ ) .....	78
5.28.Effect of the Coulomb Friction ( $M^* = 3$ .....	79
5.29.Effect of the Coulomb Friction ( $M^* = 2M$ ) .....	79
5.30.Effect of the Coulomb Friction ( $M$ ) .....	80
Fig.A Friction Model and its Analog Circuit .....	86

## NOMENCLATURE

$C_{ns}$	material damping coefficient of nut - screw assembly.
$C_{nsT}$	torsional equivalent of $C_{ns}$
$C_s$	material damping coefficient of lead - screw
$C_{TC}$	material damping coefficient of coupling
$D_{ba}$	coefficient of viscous damping at aft end bearing
$D_{bd}$	coefficient of viscous damping at drive end bearing
$D_m$	motor viscous damping coefficient
$D_{ta}$	slide viscous damping coefficient
$D_{tT}$	torsional equivalent of $D_{ta}$
$E_g$	motor back e.m.f.
$I$	current
$J_{ba}$	aft end bearing inertia
$J_{bd}$	drive end bearing inertia
$J_c$	coupling inertia
$J_m$	motor rotor inertia
$J_T$	slide inertia
$K_{as}$	axial stiffness of lead screw
$K_B$	motor back emf constant
$K_{ba}$	axial stiffness of aft end bearing
$K_{bd}$	axial stiffness of drive end bearing
$K_E$	position transducer gain
$K_{ea}$	equivalent axial stiffness of lead screw assembly
$K_{eaT}$	torsional equivalent of $K_{ea}$
$K_{ns}$	axial stiffness of screw - nut assembly
$K_{nt}$	axial stiffness of nut - slide connection
$K_P$	position loop gain
$K_T$	motor torque constant
$K_{TC}$	torsional stiffness of coupling

$K_{TS}$	torsional stiffness of screw
$K_V$	velocity loop gain
$L$	length of ball screw
$L_a$	motor inductance
$M_T$	mass of the slide
$n$	time scale factor
$P$	lead screw pitch
$R_a$	motor armature resistance
$R_T$	total resistance
$T_f$	friction torque
$T_{fm}$	motor friction torque
$T_{fs}$	slide friction torque
$T_g$	electrically generated torque
$V$	motor terminal voltage
$\theta$	angular position
$\dot{\theta}$	angular speed
$\ddot{\theta}$	angular acceleration
$w$	natural frequency
$\mu$	friction coefficient
$\tau$	compute time

## CHAPTER 1

### INTRODUCTION

The feed drive system is the most important part of nc machine tools because of direct effect on the positioning accuracy of the slide and therefore the accuracy of the workpiece. For that reason, after determining the sizes of the components of the feed drive system, the design should be finalised by checking its dynamic performance.

The feed drive system consists of an actuator, a coupling unit, a transmission unit and load. This study is mainly devoted to direct drives in which actuator is directly coupled to the transmission unit. In addition, the feed drive system is controlled by the way of position and velocity feedback. Compensation is not considered in this study.

The system is examined on a two inertia linear model. But a non-linear model including the friction is also analysed. Some researchers (2,4) indicate that the two-inertia model is sufficient to analyse the system.

Dynamic performance can be examined by either digital simulation or analog simulation. Analog simulation is more rapid than digital simulation. Low cost of analysis is also an advantage for analog computer in spite of the low accuracy, compared with digital simulation.

The aim of this thesis is to bring more organization on the work of modelling of feed drive systems and to illustrate the effect of variation of the system parameters on the dynamic performance and hence to help the designer in finding the compromise between conflicting requirements in finalising the design.

The influence of the system parameters on the dynamic performance is described by an illustrative example whose parameters are taken from a real machine tool. Stiffness, load inertia, damping coefficient, control

loop gains and friction coefficient between slide and slideway are used as system parameters.

GP - 6 Comdyna analog computer is used for this purpose.

## CHAPTER 2

### LITERATURE SURVEY

#### 2.1. INTRODUCTION

In this chapter, the most relevant literature on the work reported in this thesis is presented.

Section 2.2 is devoted to the studies on feed drive modelling. Analog simulation and its important aspects are covered in section 2.3

#### 2.2. FEED DRIVE MODELLING

An equivalent model is used in the analysis of the feed drive. Previous works (2,3) indicate that torsional model are convenient in obtaining the governing equations.

Seto and Yamada (1) have studied to improve the controllability of machine tool feed drive. They used the method of linear analysis to evaluate the performance of system. The results are represented by a special pole - zero locus graph.

Filiz (2) has developed an effective method to design and select the components of high performance machine tool feed drives. For this purpose, he has studied on the feed drive models. In his work, an interactive computer program was prepared for both of them. In addition, the design of control systems and digital simulation for the evaluation of performance was explained.

Ikawa and Mizumoto (3) have made an analysis for the transitional behaviour of the machine tool table at positioning with the aid of digital simulation. A spring - mass model with five degrees of freedom is used as an equivalent system of a typical feed drive mechanism which consists of the table, a leadscrew, a gearbox and an actuator. The



effects of the dynamic parameters of the feed drive component on the positioning accuracy are evaluated and it is shown that the model with five degrees of freedom can be simplified into the model with one or two degrees of freedom for some of the feed mechanisms with conventional structure.

Dutcher (4) has discussed the design of the servo system and different types of components of nc machine tool feed drives. He has described the effect of stiffness, friction and lost motion of the transmission unit on servo performance.

Zeleny (5) has made an analysis of the design of feed drives for nc machine tools. The stability is studied with consideration of the compliance and the backlash in the feed drive of the machine tools operating with position feedback. The regulating range of the feed rate and the possibilities of reducing the overshoot are investigated for feed drives of machine tool operating without position feedback.

Thomson (6) suggests various methods for eigen values of lumped parameter system. The basic concepts of the modelling and the analysis of spring - mass system are also examined.

Khong and Bell (7) have studied on dc motors of the feed drives for nc machine tools. They seek to clarify the design procedure. The classes of dc motor that are commercially available are discussed with the aid of tabulated performance parameters of current motors. In addition, the interaction between the power amplifier and the dc motor is presented.

Andreev (8) compares technical characteristics of some dc motors. He shows their basic advantages and disadvantages. He also specified the special advantages of high torque motors for the nc machine tools.

The dynamic and electrical equations, various characteristics, new types and selection and design criteria of dc motor are evaluated by (9). It also includes the design considerations of control system. These aspects are illustrated in various examples.

### 2.3. ANALOG SIMULATION

Analog simulation is a common way to analyse the dynamics of feed drive systems. System equations are scaled to apply to the analog computer. Previous studies pointed out the difficulties and importance of scaling.

Jackson (11) gives a very wide text on analog computation and design of computer elements. He has studied on many subjects from the basic analog computer to hybrid systems.

Rajaraman (12) explains the techniques of solving ordinary differential equations using the analog computer and for simulating systems described by ordinary differential equations. He illustrates those techniques with various examples.

Blum (13) represents the dynamic behaviour of electro - mechanical devices and systems using analog or hybrid simulation. Transient and steadystate phenomena associated with either ac or dc electrical machine have been investigated. As an example of such an application, the development and simulation of the mathematical model of an automobile alternator are given in his analysis.

Rea (14) has designed the mechanical linkages using an analog computer. The necessity to be able to assess quickly the effects of changing linkage parameters on the motion of the linkage has provided by using logical control and high speed repetitive operation.

Cuppan and Bollinger (15) have investigated a procedure for simulating the dynamic behaviour of a machine tool structure and drive system on an analog computer. The numerical values for the system parameters were taken from digital computer studies of the structure and data from component manufacturers. Various open - loop studies performed with this simulation were discussed and where it is possible, compared with experimental studies.

Benett (17) has explained the scaling on the analog computer. Especially, bootstrap technique is described as a way of effective usage of the analog computer componets. In addition he gives a software about parallel logic analog computation.

Stephenson (18) has pointed out the importance of the computers and compared the digital and analog computers and investigated the techniques for modelling and scaling with various examples.

Pessen (19) shown two rules for time scaling on analog computation. Two rules of thumb are presented for determining whether a change in time scale in the computer circuit is necessary or not. One of them is for the simulation of feedback systems by means of transfer functions and the other applies to circuits for solving differential equations.

Ashley (20) discusses the consideration errors in time scaling and suggests a different approach for time scaling. He also discusses the advantages of using the state variable notation.

Cannon (21) has proposed a systematic matrix method which may be used to scale differential equation written in state variable form. The method requires estimates of the maximum values of each computer variables and the technique is shown to be applicable to both linear and non - linear systems. The method is followed by an effective rescaling algorithm.

Auslander (22) has investigated new approaches and idea about scaling. State variable notation is used to write the equations. The scaling is done both without requiring any prior knowledge of the system's behaviour and without requiring any knowledge about the time of response. There is Just one process in preparing a set of equation for analog solution.

An analog computer circuit that correctly simulates the static and kinetic effects of dry friction is given by Wang and Shen (24). This analog computer circuit including diod function generat or satisfies the friction model. A high gain limiter and a shifted hysteresis are used in circuit so it represents the effect of the friction while the velocity approaches zero.

Parnaby (25) has studied the friction effects in a class of hydraulic servomechanisms. He has realised a circuit to satisfy the friction model. The circuit has an output which depends upon the sign of the input. The ratio of static and coulomb friction, together

with threshold velocity up to which the friction is held at the static level, are readily adjustable and its velocity can be made extremely small so as to give virtually instantaneous change from the static level to the coulomb level when input velocity changes sign.

## CHAPTER 3

### FEED DRIVE MODELLING

#### 3.1. INTRODUCTION

Feed drive model and its equations of motion will be obtained in this chapter. Lumped parameter approach is used in modelling. Both linear and non - linear models are employed for the analysis of system. Friction is used as a sole non - linear parameter in the non -linear model. The control system consists of a velocity feedback and a position feedback loop.

The section 3.2 gives the general view of modelling in feed drive systems. The models of the components of the feed drives, combination of these are presented in section 3.3. Model equations are obtained in section 3.4.

#### 3.2. THE GENERAL VIEW ON MODELLING AND FEED DRIVE

The characteristics of dynamic systems are described with their equivalent models. The equivalent models can be obtained by using two different approaches. One of them is lumped parameter approach which consists of discrete masses, springs and dashpots. Complex systems can be modelled more easily by this approach but it includes some errors because of various assumptions which are the lumping of the mass at a few discrete points, approximate friction models, etc. These errors must be kept in mind. The other one is distributed parameter method which is more exact, but analysis are limited to a narrow selection of problems, such as uniform beam and slender rod.

Lumped parameter approach is used in feed drive modelling because of ease of applicability as was pointed out by many researchers (1,2,3).

This method is applied to each component of feed drive and they are represented by a number of massless field and fieldless mass. A field is shown by spring and dashpot which represent the stiffness and damping respectively and fieldless mass defines each lumped inertia. The combination of these components gives the model of feed drive.

The vibration of system has two modes. The rotational parts and translational parts create the torsional and axial modes of vibration respectively. There is not coupling between these. To simplify the model and to ease the writing of equations of motion, axial part of the model is converted to its torsional equivalent. For pure torsional model, equations of motion are written at each lumped inertia by using Newton's second law. These are the second order ordinary differential equations.

A feed drive is a group of mechanical, electrical and hydraulic or pneumatic components that controls the position and/or velocity of a machine slide as shown in figure (3.1). An input which can be position, velocity or torque (acceleration) is given to obtain a response at slide.

The components of feed drives can be separated into four groups.

- 1) Actuator
- 2) Coupling unit
- 3) Transmission unit
- 4) Table

Actuator is used to provide the power. A dc servomotor, a stepping motor, a hydraulic motor or a hydraulic cylinder which is directly coupled to the load without transmission unit can be used as an actuator. As a result of the requirements of the machine tool about actuators, the feed drive must be capable of delivering a high torque at low speeds and a small torque at higher speeds for rapid traverse.

Coupling unit connects the actuator to the transmission unit with or without torque and speed reduction or amplification. These are supplied with a gearbox or a toothed belt or a coupling. If a coupling is used, the feed drive is called as direct drive. A coupling is used

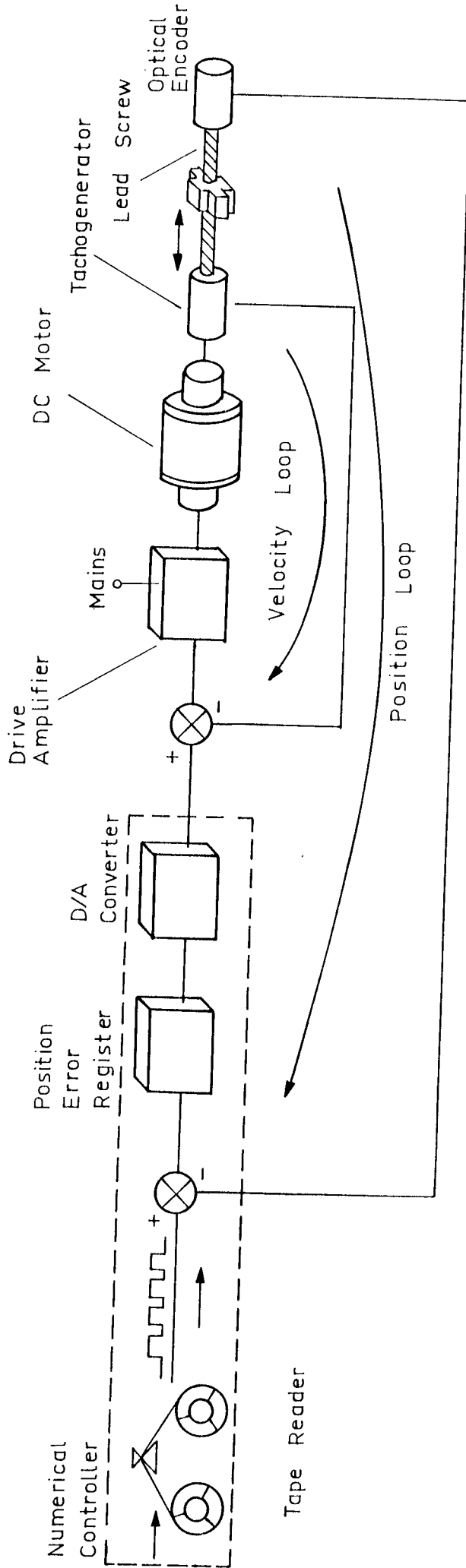


Fig.3.1 General Arrangement of a Numerical Controlled Feed Drive Axis.

as a coupling unit in this study.

Transmission unit transmits the power from a source to a load. It has a few kinds which are lead screw, rack - pinion and hydraulic cylinder which is also used as an actuator. A ball bearing screw assembly is used as a transmission unit in this study. Filiz (2) indicated that the ball bearing screw has some advantages which are the low friction, low wear, easy lubrication and high efficiency compared to lead screw.

Table carries the tool holder or the work piece. It may be moving on plain, antifriction, combined or hydrostatic slideways.

### 3.3. Modelling of Feed Drive and Deriving the Model Equations

The model of each component of feed drive is obtained independently from each other. And the combination of these at discrete points creates the feed drive model.

#### 3.3.1 DC Motor Model

The equations of armature controlled dc motor include the electrical and mechanical parameters. A dc motor model consist of an inertia, a dashpot and a generated torque,  $T_g$ , acting on the inertia. Dashpot represents the viscous damping coefficient,  $d_m$ , which is obtained from the manufacturer's catalogues.

A dc motor can be illustrated by an equivalent electrical circuit as shown in figure 3.2. The relationship between the parameters may be written as follow:

$$V = L_a \frac{dI}{dt} + R_a I + E_g \quad (3.1)$$



The motor back emf constant is proportional to rotor velocity, this relationship is expressed as :

$$E_g = K_B \cdot \dot{\theta}_m \quad (3.2)$$

Substituting the expression for  $E_g$  in to equation 3.1, then :

$$V = L_a \frac{dI}{dt} + R_a I + K_B \dot{\theta}_m \quad (3.3)$$

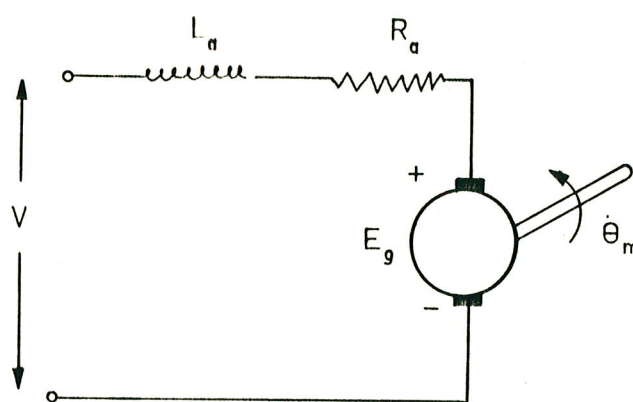


Fig.3.2 Equivalent Circuit for DC Motor

Since the magnetic field in the motor is constant, the current produces a proportional torque.  $T_g$ .

$$T_g = K_T \cdot I \quad (3.4)$$

The relationships between speed - torque and current - torque are approximately shown in figure 3.3.

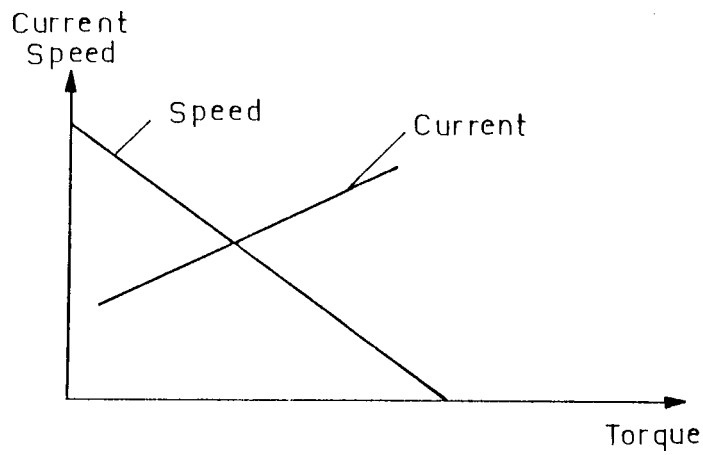


Fig.3.3 Speed - Torque and Current - Torque Curve of PM DC Motor

If the model contains the motor friction torque, it is called as non - linear model. Figure 3.4 shows the linear and non - linear model. The model of friction will be given in section 3.3.4

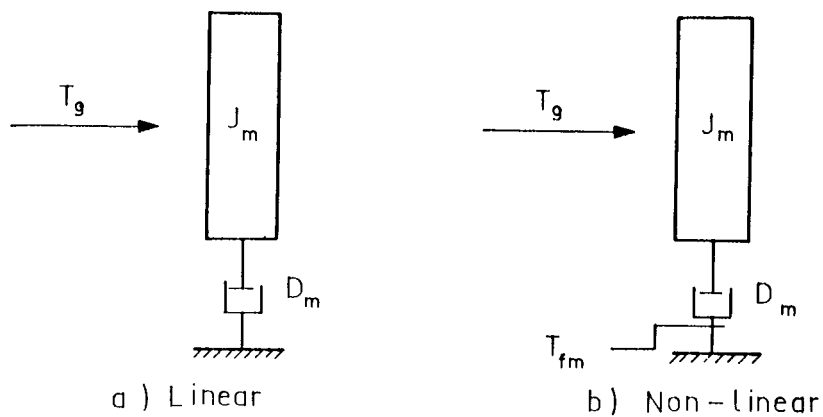


Fig. 3.4 DC Motor Models

### 3.3.2 Coupling Model

Coupling is considered as an inertialess field and two fieldless inertias. The friction between two mating part is ignored. Two fieldless inertias are assumed to equal to each other. They are expressed as :

$$J_{c1} = J_{c2} = J_c/2 \quad (3.5)$$

A coupling and its model are shown in figure 3.5.

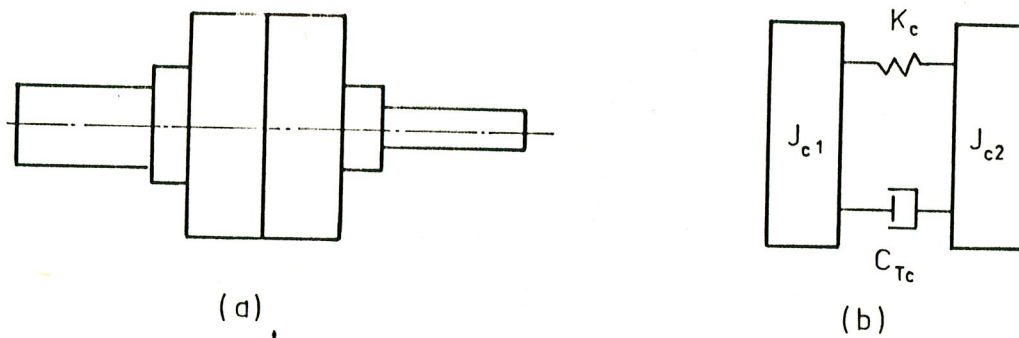


Fig. 3.5 A Coupling and its Model

The stiffness,  $K_c$ , is generally given by the manufacturers or can be calculated. The damping,  $C_{Tc}$ , represents the material hysteresis. The type of this is a flexible coupling.

### 3.3.3 Leadscrew Assembly Model

The components of system are thrust bearings, ball bearing screw, ball - nut and the machine tool slide. There are two kinds of vibration depending on rectilinear motion and rotation. Rectilinear motion is composed of motion of slide and ball - nut. Rotation consists

of motion of ball bearing screw and thrust bearings. After torsional and axial model are constructed, axial model is converted to its torsional equivalent so the model is represented by a pure torsional model.

### 3.3.3.1 Torsional Model

This model is obtained according to the supporting method. If double ended assembly is used, then 3 discrete points are chosen. These are at the drive end, at the nut point and at the aft end. In this assembly, drive end and aft end are equipped with thrust bearing and this supporting method can be considered as both end fixed. If single ended assembly is used, then 2 discrete points are chosen. These are at the drive end and at the nut point respectively. In this case, thrust bearings are placed at the drive end and they carry axial load in both direction. This supporting method can be expressed as one end fixed and the other end simply supported. The schematic representation of these assemblies and their models are given in figure 3.6 and 3.7 respectively.

The determination of the model parameters is given as follows :

#### a) Inertia

$J_s$  is the total inertia of the screw. If the distance ,x, between point 1 and point 2 is described as a variable, inertias at each discrete point are expressed as follows :

For Double Ended Assembly

$$\begin{aligned}
 J_{s1} &= 0.5 J_s \frac{X}{L} \\
 J_{s2} &= 0.5 J_s \\
 J_{s3} &= 0.5 J_s \frac{L - X}{L}
 \end{aligned}
 \tag{3.6}$$

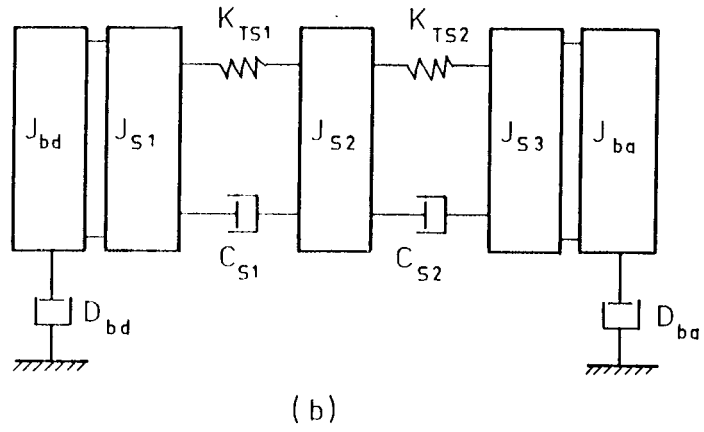
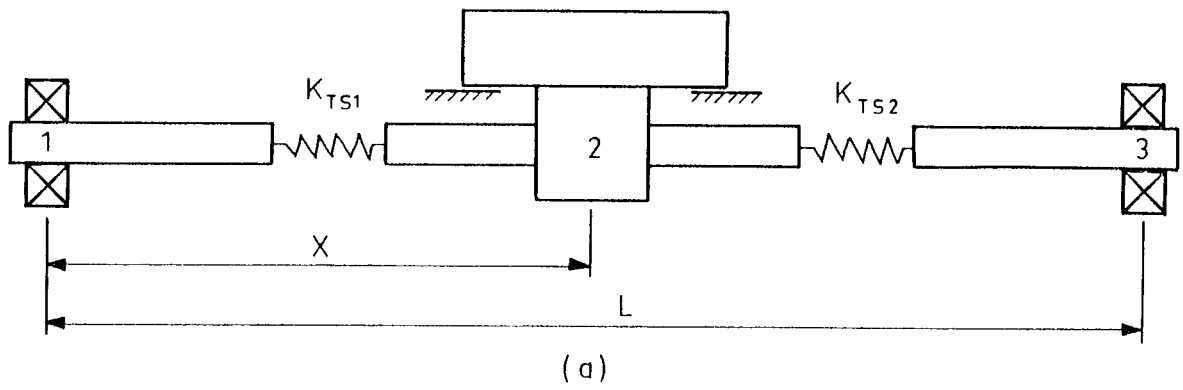


Fig. 3.6 Double Ended Leadscrew Assembly Configuration and its Model.

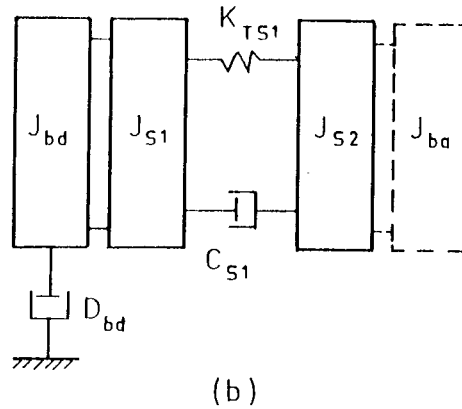
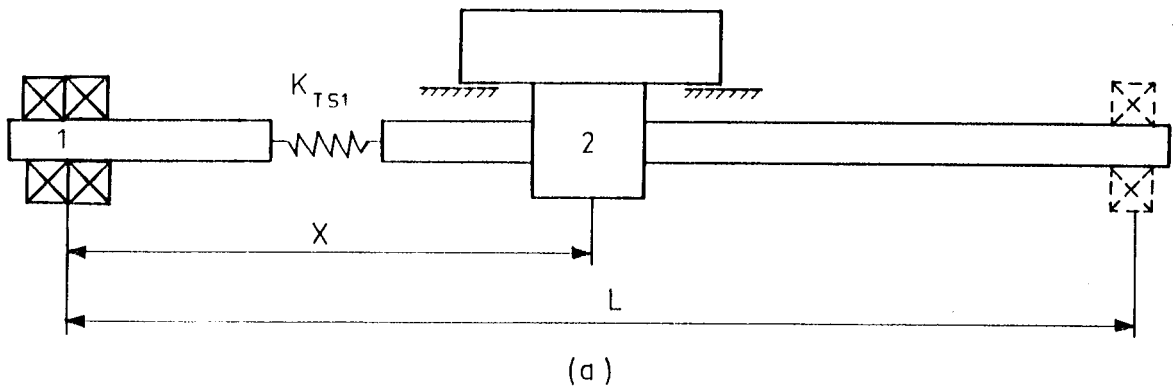


Fig. 3.7 Single Ended Leadscrew Assembly Configuration and its Model.

$$J_1 = J_{bd} + J_{s1}$$

$$J_2 = 0,5 J_s \quad (3.7)$$

$$J_{s3} = J_{ba} + J_{s3}$$

where  $J_{s2}$  is always  $0,5 J_s$

For Single Ended Assembly

$$J_{s1} = 0,5 J_s \frac{X}{L}$$

$$J_{s2} = J_s - J_{s1} \quad (3.8)$$

$$J_1 = J_{bd} + J_{s1} \quad (3.9)$$

$$J_2 = J_{s2} + J_{ba}$$

If the supporting method of ballscrew is one end fixed and one end free, then  $J_{ba}$  disappears in equation (3.9).

#### b) Torsional Stiffness

If the torsional stiffness of the screw is  $K_{TS}$ , the distribution of the stiffness between discrete points is as follows :

For Double Ended Assembly

$$K_{TS1} = K_{TS} \frac{L}{X} \quad (3.10)$$

$$K_{TS2} = K_{TS} \frac{L}{L - X}$$

For Single Ended Assembly

$$K_{TS1} = K_{TS} \frac{L}{X} \quad (3.11)$$

### c) Damping

The damping in the leadscrew results from material hysteresis losses. In addition the damping depending on the lubrication is called viscous damping which is between inertias and ground. It depends on the various operating conditions.

#### 3.3.3.2 Axial Model

Axial model of the ball bearing screw assembly is the most important part of the feed drive modelling. Because the torsional equivalent of axial stiffness is much lower than torsional stiffnesses. So it strongly affects the system performance and lost motion and results in a lower resonant frequency.

The effective mass in the model is the mass of slide including the mass of the nut. Equivalent stiffness of axial model is composed of the axial stiffnesses of the bearings  $K_{bd}$  and  $K_{ba}$ , nut - table connection,  $K_{nt}$ , nut - screw connection  $K_{ns}$  and the screw,  $K_{as}$ , for its whole length. The stiffness of bearing housing is ignored because of its high value.

#### For Double Ended Assembly

The double ended configuration of leadscrew assembly including its axial model parameters is illustrated in figure 3.8. The axial stiffnesses of the screw shown in that figure are expressed as :

$$K_{asl} = K_{as} \frac{L}{X} \quad (3.12)$$

$$K_{as2} = K_{as} \frac{L}{L - X}$$

The combination of these axial stiffnesses creates the equivalent stiffness. If the bearings of the ball bearing screw are identical then  $K_{asl} = K_{as2} = 2K_{as}$  and  $K_{nt}$  is assumed to be higher than  $K_{ns}$ , so  $K_{ea}$  is expressed as :

$$K_{ea} = \frac{K_{bd} K_{as} K_{ns}}{4K_{bd} K_{as} + K_{bd} K_{ns} + 2K_{as} K_{ns}} \quad (3.13)$$

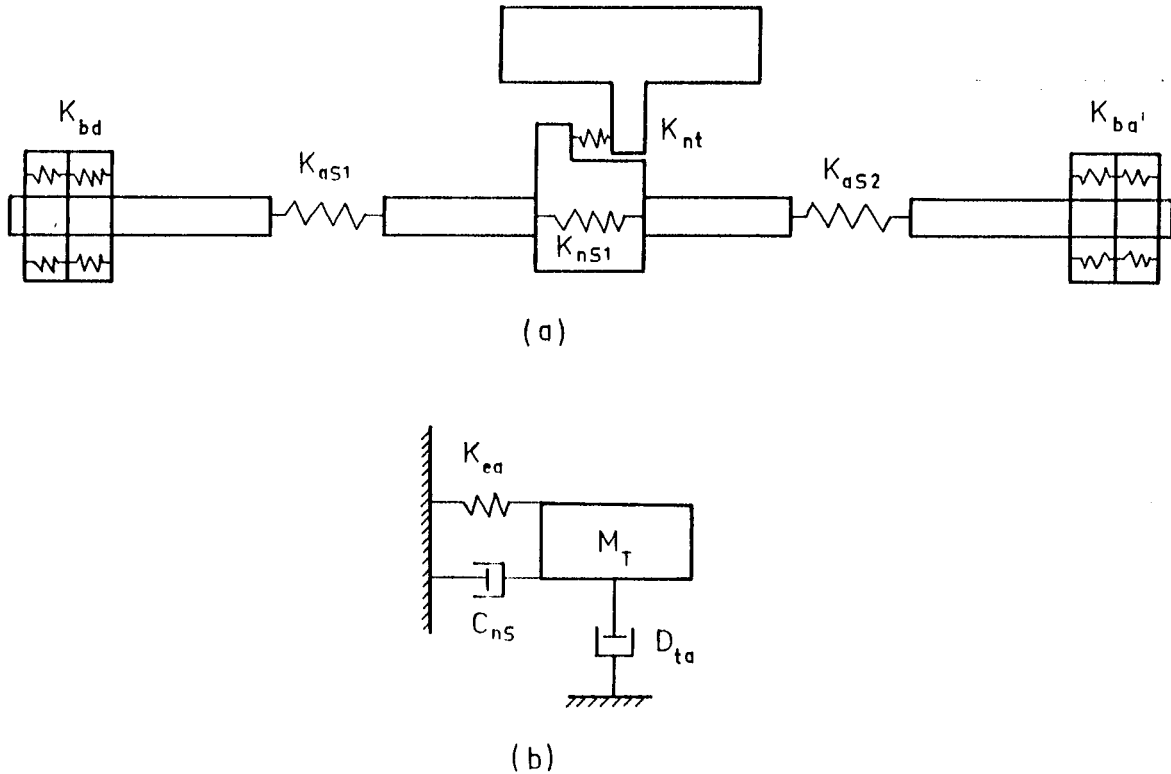


Fig. 3.8 Axial Model of Double Ended Leadscrew Assembly

where  $C_{ns}$  is the material damping of nut - screw connection and  $D_{ta}$  is the viscous damping on the slideway surfaces.

At the double ended assembly, the equivalent stiffness is lowest at the middle of ball bearing screw.

#### For Single Ended Assembly

The single ended configuration of lead screw assembly including its axial model parameters is illustrated in figure 3.9. In this model,  $K_{as2}$  and  $K_{ba}$  are assumed to be zero. And then the combination of stiffness terms creates the equivalent stiffness. It is expressed as :



$$K_{ea} = \frac{K_{bd} K_{asl} K_{ns}}{K_{bd} K_{asl} + K_{bd} K_{ns} + K_{asl} K_{ns}} \quad (3.14)$$

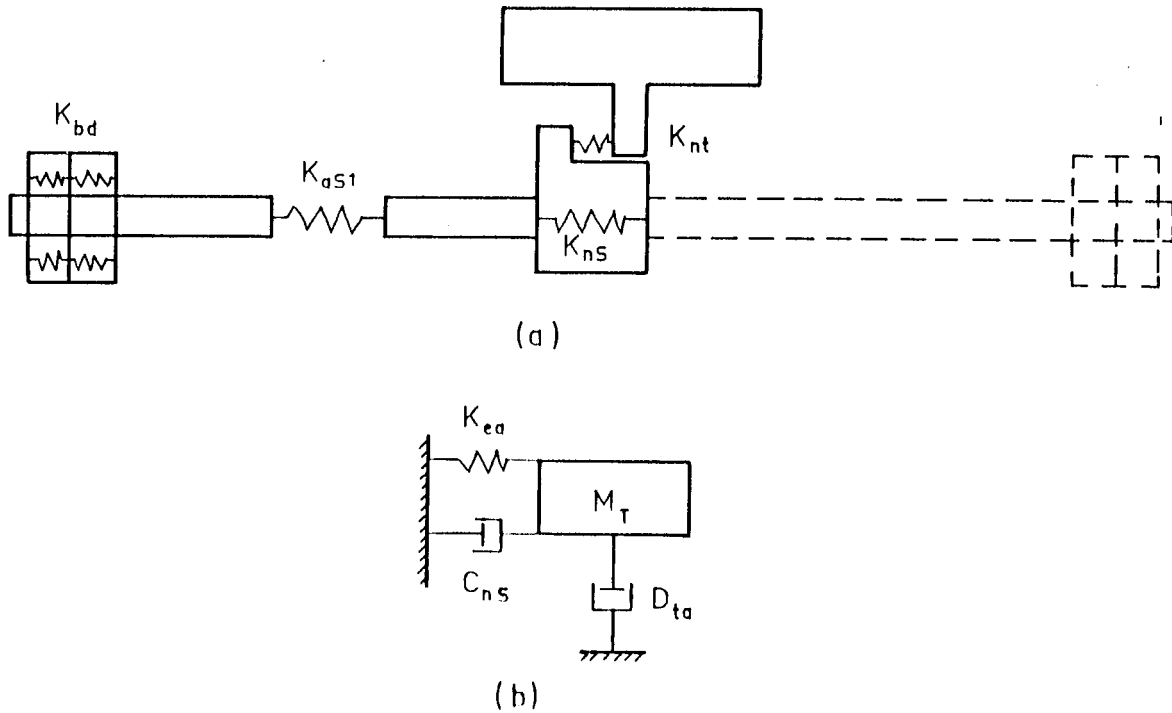


Fig.3.9 Axial Model of Single Ended Leadscrew Assembly

The equivalent stiffness has the lowest value at the stroke position from the drive end for the single ended assembly.

If all parameters in axial models are multiplied by  $(P/2\pi)^2$  to obtain their equivalent torsional model, the feed drive model can be constructed by pure torsional parameters. Torsional equivalent of axial models is shown in figure 3.10. This is true for both single ended and double ended assembly. But parameters are different from each other

The torsional model and the torsional equivalent of axial model of leadscrew are combined at the nut point because the rotary motion is converted to rectilinear motion through the nut. This model is also combined with dc motor and coupling model and so feed drive model is

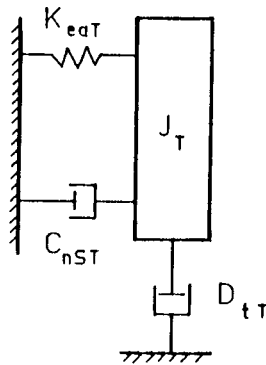


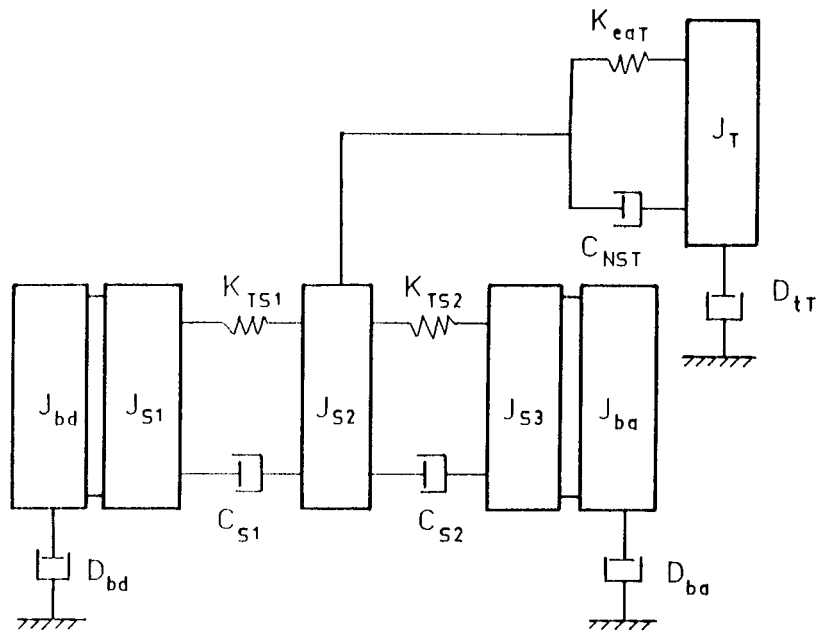
Fig. 3.10 Torsional Equivalent of Axial Models

obtained. The combined models of leadscrew are illustrated in figures 3.11(a) and 3.11(b). If the friction is included in model, then it is called as non-linear model. These models are shown in figure 3.12(a) and 3.12(b). The feed drive models are represented in figure 3.13 and 3.14.

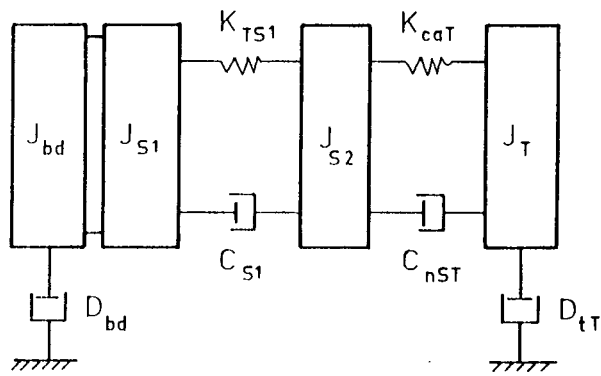
#### 3.3.4 Friction Model

Friction is the resistance that is encountered where two elements' surfaces slide or tend to slide over each other. These surfaces can be dry or lubricated. In the first case, friction is called as dry friction. The second case is out of the scope of this study. Therefore it is not included here.

If a force is applied to an element, it tends to slide. But friction force is resisted up to a definite value of applied force, that value is equal to maximum static friction force. When force reaches to that value, element earns a very small velocity so that friction force instantly drops to a low value which is called kinetic friction force and motion starts. This velocity is also called as threshold velocity. This phenomena is illustrated in figure 3.15(a). But it is represented with torque and angular velocity in stead of force and linear velocity. The analog circuit of this model is given in appendix. But it is not

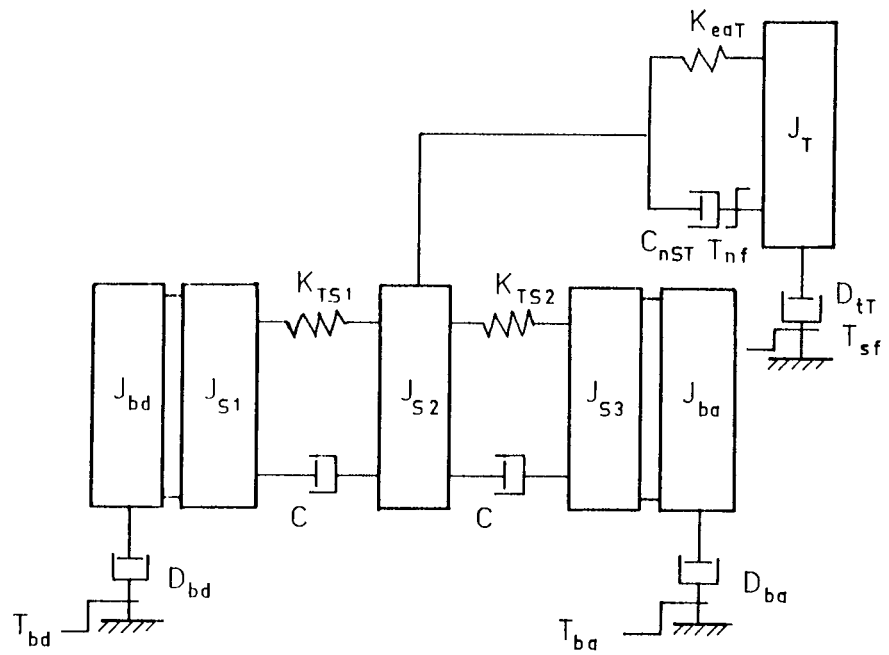


a) Double Ended

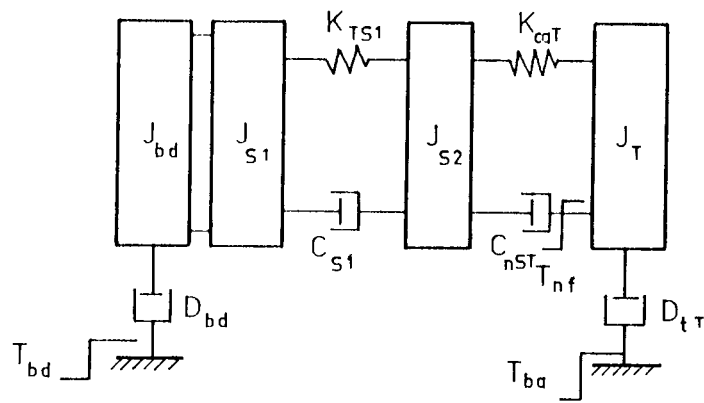


b) Single Ended

Fig.3.11 Combined Model of Leadscrew Assemblies.

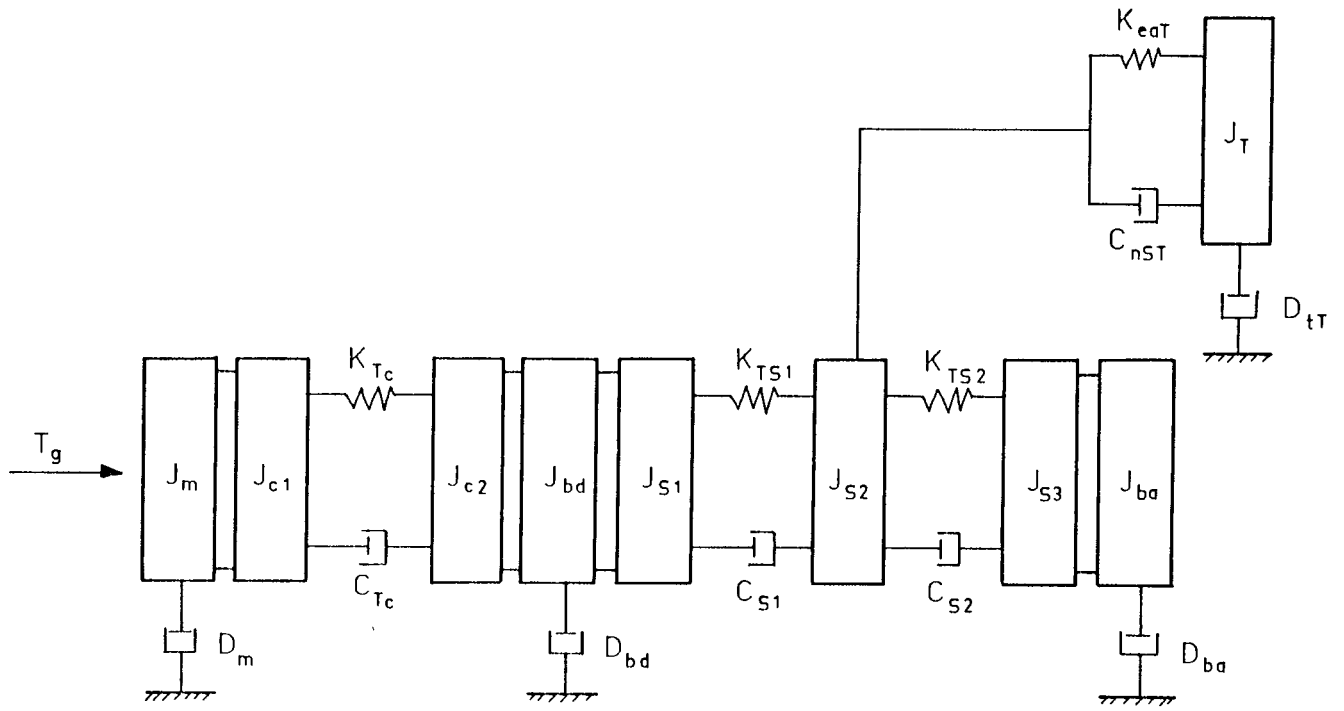


a) Double Ended

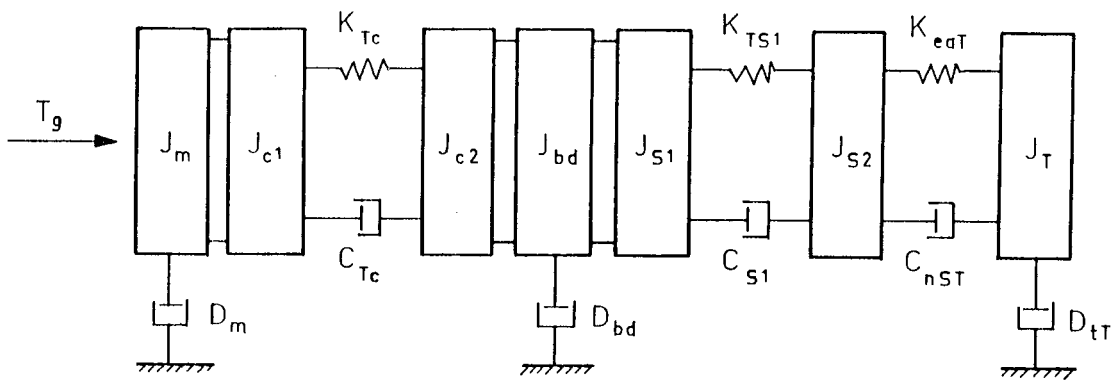


b) Single Ended

Fig.3.12 Combined Non-Linear Model of Leadscrew Assemblies.

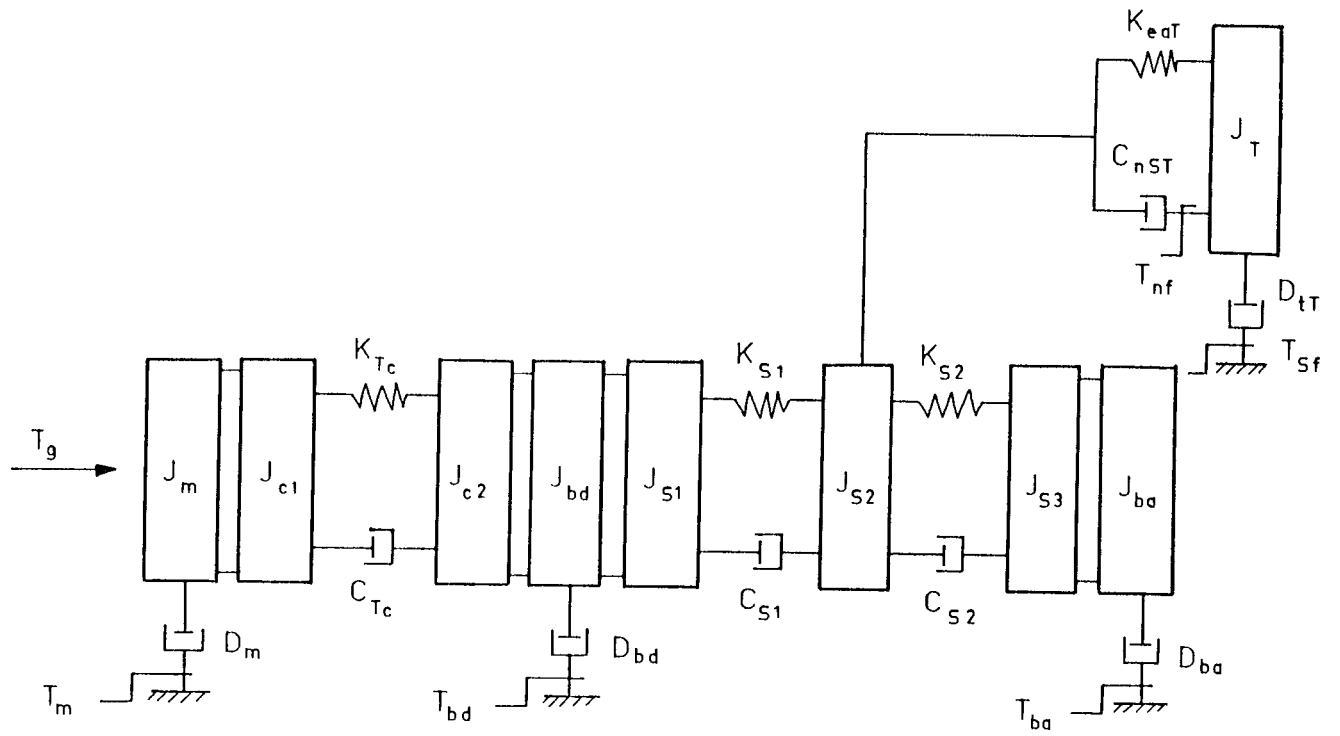


a) Double Ended

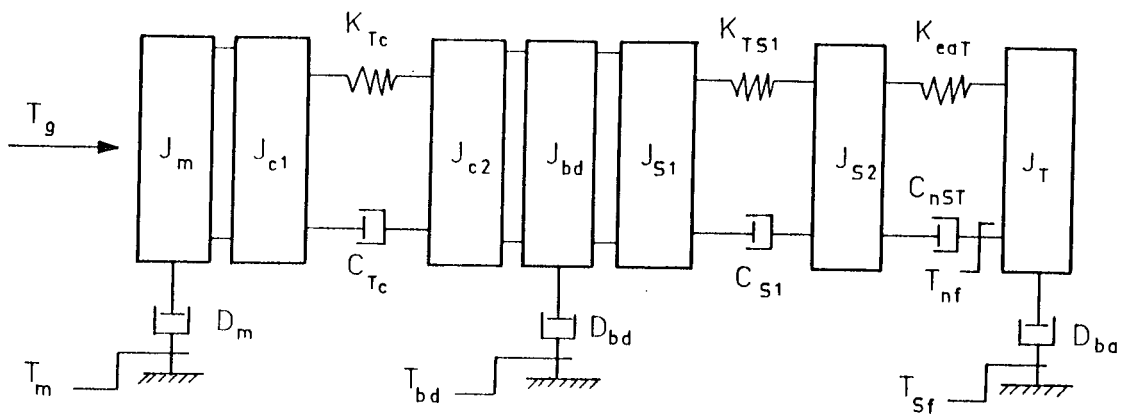


b) Single Ended.

Fig.3.13 Linear Models of Feed Drive.



a) Double Ended.



b) Single Ended.

Fig. 3.14 Non-Linear Models of Feed Drive.

used in this study. This model is simplified as shown in figure 3.15(b). It only includes the kinetic friction. This model is used as a friction model in this study. Analog circuit of it is included in chapter 4.

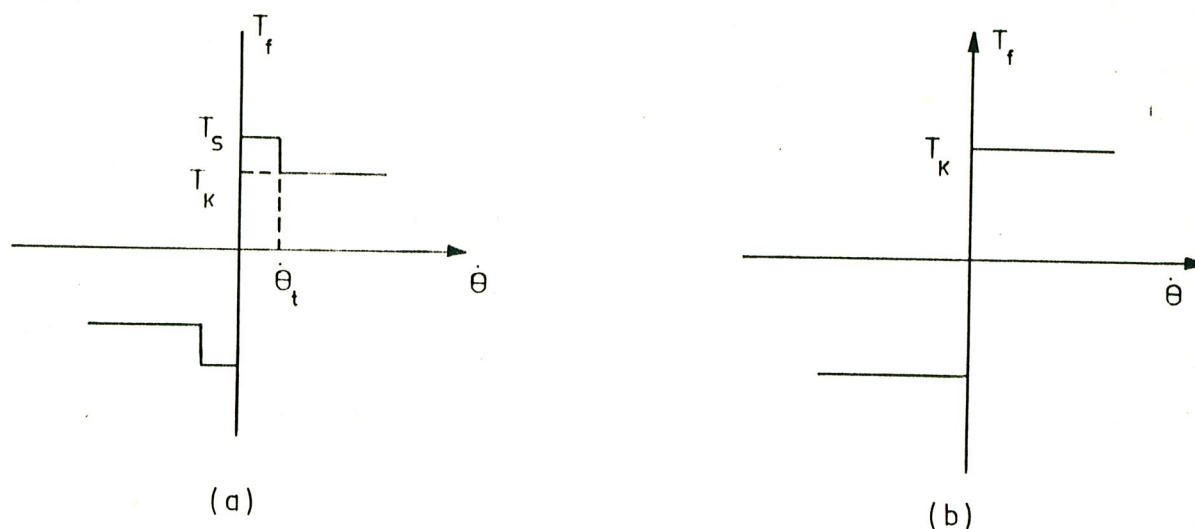


Fig.3.15 Friction Models

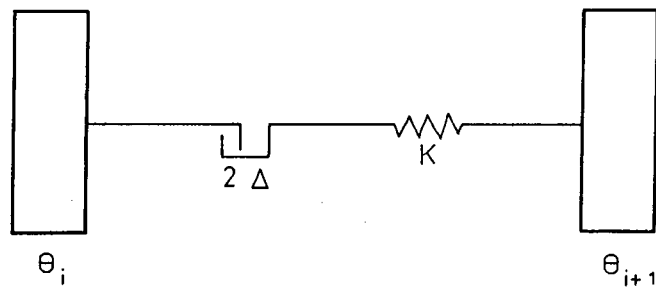
### 3.3.5 Backlash and its Model

Although backlash and its model are out of the scope of this study, it is included here for the sake of the completeness of the model.

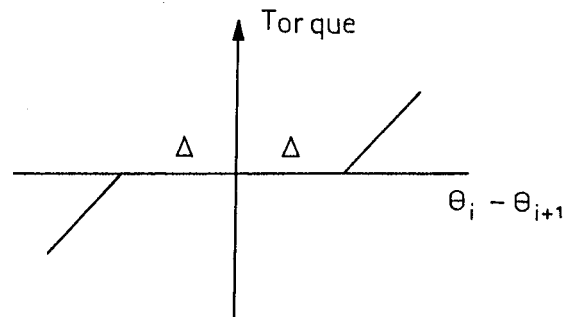
Backlash can be expressed as looseness between mating parts operating together. In a feed drive, backlash includes any looseness in the

bearing mounting, end play of the screw, looseness between screw and nut, and looseness in the nut mounting. These cause to the limit cycle oscillations because of the impact between two inertias. But, in many N.C. machine tools, the backlash are reduced to the very small values (total 0,005 mm or less). This is provided in nut and screw and bearings with preload. The use of ball - bearing lead screws with two preloaded ball nuts essentially eliminates backlash between the screw and the nut. Preloaded double thrust bearings are certainly required on at least one end of the screw to eliminate the backlash. The model of the backlash is represented in figure 3.16 which had been taken from Filiz (2).

$\Delta$  represents the looseness.



(a)



(b)

Fig. 3.16 Backlash Representation and its Model

### 3.4 MODEL EQUATIONS

The model equations are developed in this section. They are used to construct the analog simulation diagram at the next chapter. The dynamic equations of mechanical parts for five and two inertia models are written and motor equations are rearranged. The algebraic equations of control loops are derived to close the loops.

The normalised block diagram of position control system with unity feedback is illustrated in figure 3.17. Where  $G_{LM}$  gives the relationship between position of the rotor and table as radian.  $K_p$  and  $K_v$  are the position and velocity loop gains respectively.  $K_E$  represents the position transducer gain.

The algebraic equations of control loops are written as :

$$B = A - \theta_2 \quad (3.15)$$

$$C = B K_p - \dot{\theta}_1 \quad (3.16)$$



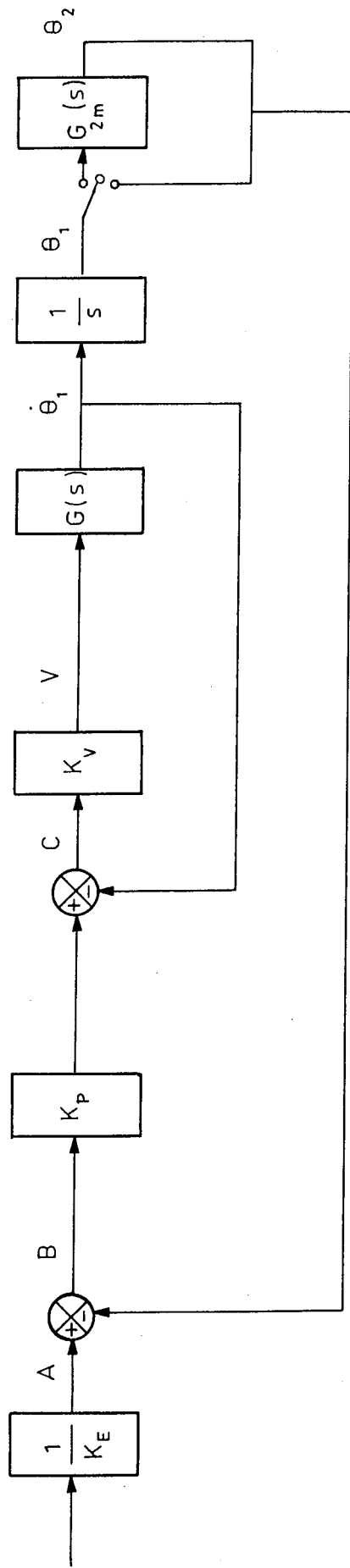


Fig. 3.17 Normalised Block Diagram of Position Control System With Unity Feedback.

$$V = C K_V \quad (3.17)$$

If position loop is closed from motor, then  $\theta_2$  is replaced with  $\theta_1$  in equation 3.15

The motor equations are rearranged in the following :

$$\dot{I} = \frac{V}{L} - \frac{R}{L} I - \frac{K_B}{L} \dot{\theta}_1 \quad (3.18)$$

$$T_g = K_T \cdot I$$

$T_g$  is identical with equation 3.4

The lumped inertias in figure 3.13 are combined to obtain the five inertia model for the double ended assembly. This model is illustrated in figure 3.18.

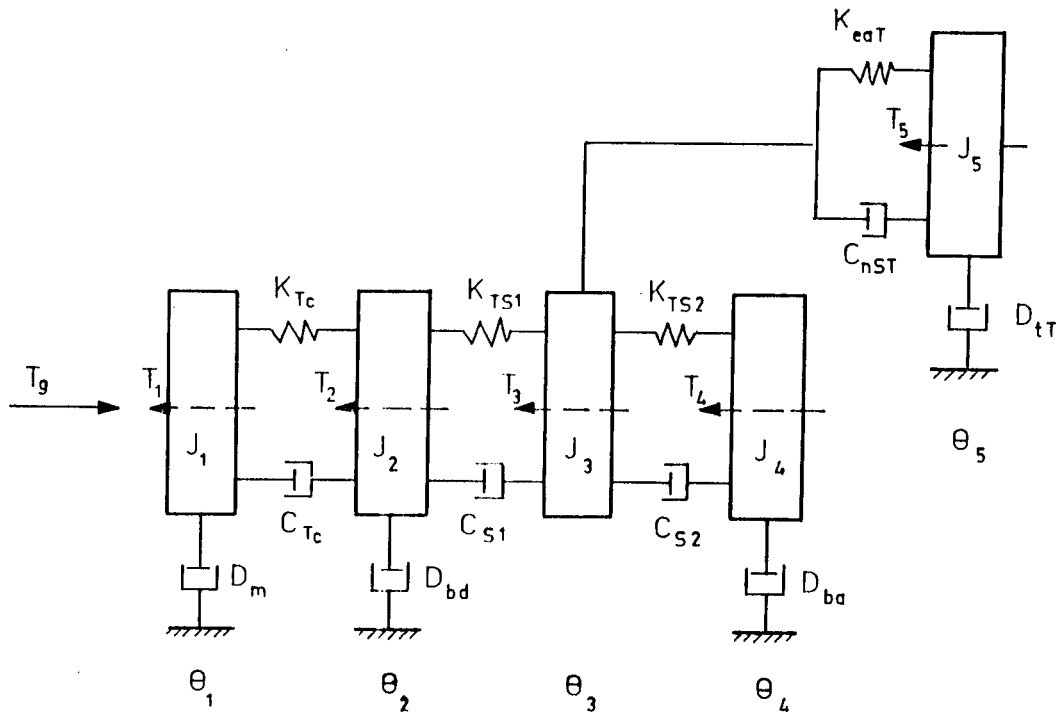


Fig. 3.18 Five Inertia Model of the Feed Drive

Where the  $J_1, J_2, J_3, J_4$  and  $J_5$  is that :

Table 3.1 Inertias of the Five Inertia Model

$J_1 = J_m + J_{c1}$
$J_2 = J_{c2} + J_{bd} + J_1$
$J_3 = J_{s2}$
$J_4 = J_{s3} + J_{ba}$
$J_5 = J_T$

The equations are written for each lumped inertia and given in equation 3.20 in the matrix form.

$$J \ddot{\theta} = D \dot{\theta} + K \theta + T \quad (3.19)$$

The coefficient matrices are those :

$$J = \begin{vmatrix} J_1 & J_2 & J_3 & J_4 & J_5 \end{vmatrix} \quad (3.20)$$

$$D = \begin{vmatrix} -(D_m + C_{Tc}) & C_{Tc} & 0 & 0 & 0 \\ C_{Tc} & -(C_{Tc} + D_{bd} + C_{s1}) & C_{s1} & 0 & 0 \\ 0 & C_{s1} & -(C_{s1} + C_{s2} + C_{nsT}) & C_{s2} & C_{nsT} \\ 0 & 0 & C_{s2} & -(C_{s2} + D_{ba}) & 0 \\ 0 & 0 & C_{nsT} & 0 & -(C_{nsT} + D_{tT}) \end{vmatrix} \quad (3.21)$$

$$K = \begin{vmatrix} -K_{Tc} & K_{Tc} & 0 & 0 & 0 \\ K_{Tc} & -(K_{Tc} + K_{Ts1}) & K_{Ts1} & 0 & 0 \\ 0 & K_{Ts1} & -(K_{Ts1} + K_{Ts2} + K_{eaT}) & K_{Ts2} & K_{eaT} \\ 0 & 0 & K_{Ts2} & -K_{Ts2} & 0 \\ 0 & 0 & K_{eaT} & 0 & -K_{eaT} \end{vmatrix} \quad (3.22)$$

$$T = \begin{bmatrix} T \\ g \\ 0 \\ 0 \\ 0 \\ 0 \end{bmatrix} \quad (3.23)$$

The stiffness values of the feed drive components of using machine tool in chapter 5 are given by (2) as follow :

Table 3.2 Stiffness Values in the Five Inertia Model

$K_{Ts1}$	=	71708 Nm/rad
$K_{Ts2}$	=	119513 Nm/rad
$K_{Tc}$	=	110000 Nm/rad
$K_{eaT}$	=	1136 Nm/rad

As shown in table 3.2, the stiffnesses of the ball bearing screw and the coupling are very much higher than the torsional equivalent of axial stiffness of ball bearing screw assembly. Therefore first, second, third and fourth inertias are considered as rigid, so the model can be reduced to a two inertia model. Filiz(2) and Ikawa and Mizumoto (3) have represented the validity of two-inertia model. The Lumped inertias for two inertia model are given in table 3.3 and the model is illustrated in figure 3.19.

Table 3.3 Inertias of the Two Inertia Model

$J_1 = J_m + J_{c1} + J_{c2} + J_{bd} + J_{s1} + J_{s2} + J_{s3} + J_{ba}$
$J_2 = J_T$

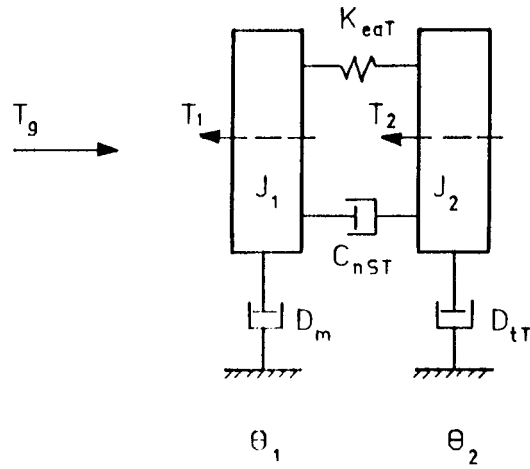


Fig.3.19 Two Inertia Model of Feed Drive

The equations of two inertia model are those

$$J = \begin{vmatrix} J_1 & J_2 \end{vmatrix} \quad (3.24)$$

$$D = \begin{vmatrix} -(D_m + C_{nsT}) & C_{nsT} \\ C_{nsT} & -(D_{tT} + C_{nsT}) \end{vmatrix} \quad (3.25)$$

$$K = \begin{vmatrix} -K_{eaT} & K_{eaT} \\ K_{eaT} & -K_{eaT} \end{vmatrix} \quad (3.26)$$

$$T = \begin{vmatrix} T_g \\ 0 \end{vmatrix} \quad (3.27)$$

The non - linear equations for non - linear two inertia model contain friction torques at motor bearings and between slide and slideway, Sign of  $\dot{\theta}$  represents the direction of the friction torque. These equations are expressed as follow :

$$J = \begin{vmatrix} J_1 & J_2 \end{vmatrix} \quad (3.28)$$

$$D = \begin{vmatrix} -(D_m + C_{nsT}) & C_{nsT} \\ C_{nsT} & -(D_{tT} + C_{nsT}) \end{vmatrix} \quad (3.29)$$

$$T = \begin{vmatrix} T_g & -\text{Sign } \dot{\theta}_1 & T_{fm} \\ 0 & -\text{Sign } \dot{\theta}_2 & T_{fs} \end{vmatrix} \quad (3.31)$$

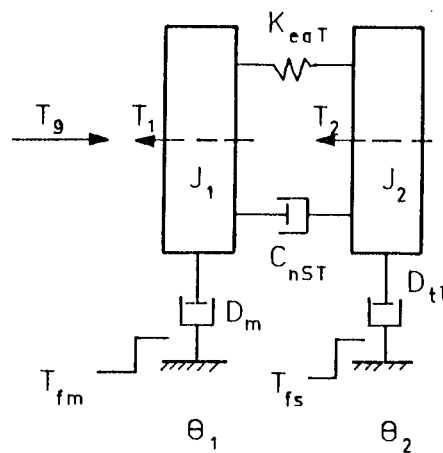


Fig. 3.20 Two Inertia Non - Linear Model

## CHAPTER 4

### ANALOG SIMULATION

#### 4.1 INTRODUCTION

Analog simulation is a powerful method in theoretical analysis of systems. The important concepts and tools of analog simulation are examined in this chapter.

Section 4.2 gives a summary about analog simulation. Analog computer components are described in section 4.3. The aim of the magnitude and time scaling and scaling methods are explain in the section 4.4. Dynamic equations are scaled and analog computer diagrams are drawn in the section 4.5.

#### 4.2 ANALOG SIMULATION

simulation means to construct a model similar to the real system so that it approximately includes the behaviour of the system. Engineers and researchers generally use models to analyse the systems. If mathematical relationships can be found to represent the behaviour of the system, these relationships can often be expressed depending on the rules of mathematics.

An analog computer model can be constructed by using the mathematical model. The model and the real system are described by the similar mathematical relationships. In analog computers, the measurable quantities are varying voltages with time although corresponding quantities of the simulated system can be displacement, velocity acceleration and etc. These voltages are easily measured and recorded but to measure and record variables of real system is not easy. In addition, non - linearities are easily simulated in analog computer.

While the behaviour of a system is studied with an analog computer model, the voltages at various point in the model behave similar to the variables of real system. It is possible to operate the system more slowly or rapidly depending on the time constant of amplifiers. Magnitude scaling is necessary when the physical limitations of the simulator prevent to give similar value for both system variables and analog computer outputs. The results of simulation are generally displayed on an oscilloscope or on a X - Y recorder.

#### 4.3 ANALOG COMPUTER

The analog computer is basically a collection of electronic parts which are operational amplifiers capacitors, resistors, potentiometers and some logic circuits. The combination of these parts gives various elements of analog computer.

The capacity of an analog computer depends on the number of operational amplifiers. Operational amplifier can be used as an inverter, summer or integrator depending on the feedback net work (element) which is either capacitor or resistor. If the feedback element is a resistor, then amplifier operates as a summer. If input and feedback resistors are identical it operates as an inverter. When the feedback element is a capacitor, Then operational amplifier operates as an integrator. The schematic representation of these cases are illustrated in figures 4.1 - 4.4

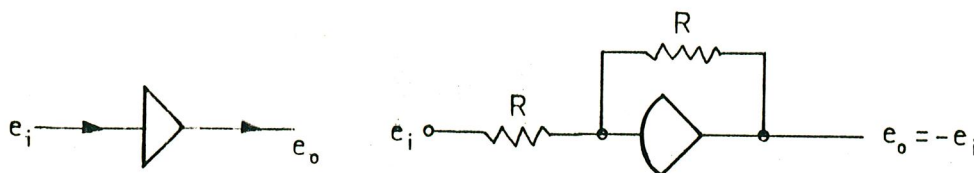


Fig. 4.1 An Analog Inverter



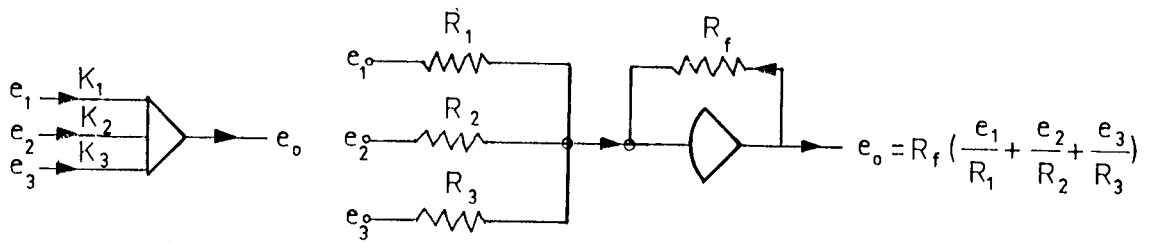


Fig. 4.2 Summer

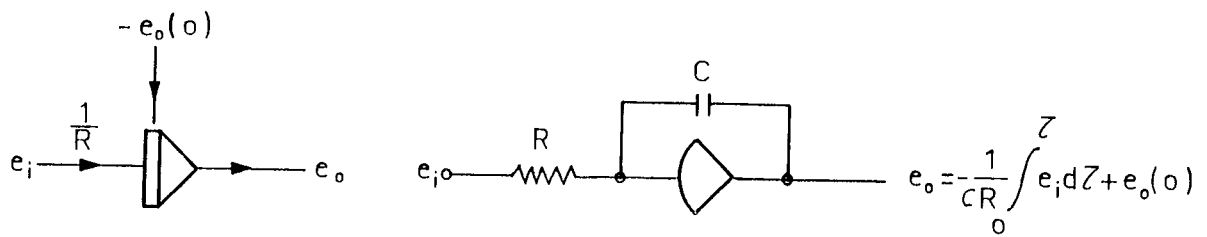


Fig. 4.3 Integrator

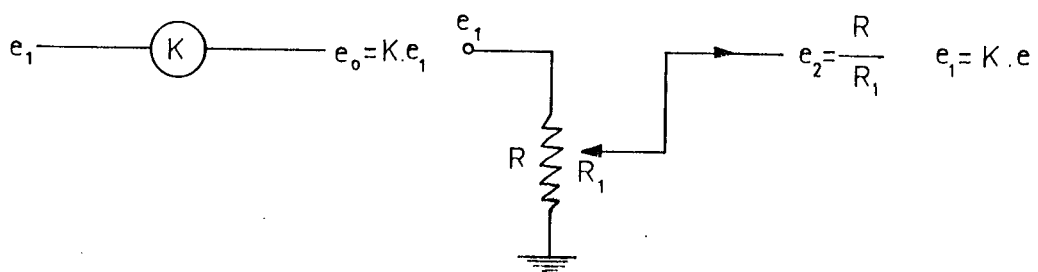


Fig. 4.4 Potentiometer

The gain of the amplifiers is calculated from the proportion of the feedback element to the input resistor. In addition, an operational amplifier always changes the sign of input signals.

#### 4.4 MAGNITUDE AND TIME SCALING

There are two kinds of scaling in analog computer work, time scaling and amplitude scaling. The necessity of the scaling arises to fit the limitations of the computer and associated recording equipment due to the requirement of the simulation system.

##### 4.4.1 Time Scaling

Time measurements of the physical systems would be in terms of micro seconds or days. If the trajectory of a bullet is studied, the time of flight will be a small fraction of a second. Whereas the time of a chemical reaction can be several days. But there are very definite limitations on the length of time about computer solution. These limitations influence the choice of time scale. These are the speed of the computer components and the recording apparatus, uncontrolled changes in the machine variables and the economic requirements. The speed of the computer components refers to the ability of a computing component to follow rapid changes in its input.

Considering these factors, an adequate time scale factors is chosen. So the solution time can be decreased or increased. The product of time scale factor and real time is equal to compute time. This relationship is expressed as :

$$\tau = n.t \quad (4.1)$$

where ;

$\tau$  : Compute time  
 $t$  : Real time  
 $n$  : Time scale factor

There are two different methods for the time scaling. One of them is to change the time scale of the model. In this method, all time terms are replaced by  $\tau/n$ . With this method, the initial conditions as well as the equations must be transformed. The other one is to change the values of RC or gains of amplifiers. So computer can operate faster or slower. The second method is generally more powerful than the first method. However there is a limitation in this method. If the amplifiers do not have capacity for sufficient gain then large time scale factor can not be applied. In this study we are going to use the first method. It is simply illustrated in a differential equation as follow :

$$\frac{d^2 x}{dt^2} + A \frac{dx}{dt} + Bx = F(t)$$

If  $t$  is replaced by  $\tau/n$ , then the differential equation is expressed as :

$$n^2 \frac{d^2 x}{d\tau^2} + A \cdot n \frac{dx}{d\tau} + Bx = F\left(\frac{\tau}{n}\right)$$

Where the variables are the computer variable. The relationship between computer variables and equation variables are given as :

$$\begin{aligned} X_c(\tau) &\equiv X(t) \\ \dot{X}_c(\tau) &\equiv \frac{1}{n} \dot{X}(t) \\ \ddot{X}_c(\tau) &\equiv \frac{1}{n^2} \ddot{X}(t) \end{aligned}$$

Where the subscript  $c$  means computer.

The magnitudes of the initial conditions and the maximum values for

variables and their derivatives change with time scale factor, but the resultant values on the potentiometer do not change.

The estimation of the time scale factor can be done in different ways. These methods are explained by Jackson (11) and Rajaraman (12). The simplest way is given by Rajaraman (12). This method is used in

1- The ratio of the coefficients of the lowest and highest order derivatives of the given differential equation is found. This ratio is  $W_n^2$ .  $W_n$  is the undamped natural frequency.

2- If this ratio  $W_n^2$  lies between 1 and 10 the equation does not require time scaling. If  $W_n^2$  is outside this range then transform the independent variable  $t$  to a variable  $\tau$  by  $t = \tau/n$ . The time scale factor  $n$  is chosen to make the ratio  $W_n^2$  in that range.

3- The transformed equation is now solved with the new independent variable .

4- The transformation  $t = \tau/n$  should be applied whenever the variable  $t$  appears in the original equation. In particular, all initial conditions and the inputs should be transform.

#### 4.4.2 Magnitude Scaling

Magnitude or amplitude scaling is done to prevent the exceeding of the reference voltage of amplifiers.

There are two different methods for magnitude scaling. These are the normalized variables method and scale factors with dimensional units. These are explained as follows.

The variables of the equation are defined as the ratio of the equation prime variable to the expected maximum value. These new variables are called scaled variable. If the variables of the system equations are substituted with scaled variables, new equation is called as scaled equations and maximum values are called as scale factor. But

to keep the system identical each variable is multiplied with its expected maximum value. Reference voltage of the computer is accepted as a unit voltage. The output of the amplifier is multiplied reference voltage and the real voltage is obtained.

The second method has the same procedure the only difference is, the scale factor is derived from ratio of reference voltage to the expected maximum value. So that the output of the amplifier directly gives real voltage.

The application of these methods to the system equations is explained by a step by step procedure as follows :

1- An unscaled diagram of the system equations are drawn. It is proper to put a potentiometer in every operational amplifier input.

2- The expected maximum values of all system variables and their derivatives are estimated. While the maximums are estimated, the knowledge about system for a well initiation can be used.

3- The scale factor using the maximums according to the using method is calculated

4- The scale factors are applied to each related variable and scaled equations are written by using system equations.

5- The block diagram are drawn by using the scaled equations and the potentiometers and the gain of amplifiers are adjusted.

6- The block diagram is patched on the computer.

7- The checking procedure is applied to prevent the various errors.

#### 4.4.3 Estimation of Maximum Values

Maximum values of the physical variables are necessary to scale the equations. There are a few approaches to obtain the maximum values. One of them is to find the maximums by using the analytic solution of differential equations. This method is generally applied to second order differential equations. And the other method is called equal coefficient rule. In fact, exact values for maximums are not necessary. The aim of estimation is essentially to get a starting value. A table was given to des-

cribe the maximum values by Rajaraman (12) for the first method. The second method is explained by a linear  $n^{\text{th}}$  order differential equation as follows :

$$a_n \frac{d^n x}{dt^n} + a_{n-1} \frac{d^{n-1} x}{dt^{n-1}} + \dots + a_1 \frac{dx}{dt} + a_0 x = F(t) \quad (4.2)$$

The equal coefficient rule is explained by a step by step procedure as follows:

1- Each term of differential equation is normalised by following constants.

$$\left( \frac{d^n x}{dt^n} \right)_{\max}, \left( \frac{d^{n-1} x}{dt^{n-1}} \right)_{\max}, \dots, \left( \frac{dx}{dt} \right)_{\max}, x_{\max} \text{ such that}$$

$$a_n \frac{d^n x}{dt^n}, \dots, a_1 x_m, a_0 x_m \text{ and nonhomogenous part are nearly}$$

equal.

2- Initial conditions are normalised by using the normalising constants determined in the previous step. If the magnitudes of scaled variables are less than unity, the above operation is repeated and it is applied to the initial conditions.

3- The sequence of normalizing constant must be a monotonically increasing or decreasing sequence. If they don't form such a sequence modify the values of the pertinent constants to ensure monotonically.

4- These constants are used to normalised the equations.

When system has a forcing function,  $a_0 x_m$  is double the magnitude of the other coefficient.

A simple example to represent the Equal Coefficient Rule.

Example 1:

$$10 \ddot{x} + 40 \dot{x} + 100 x = 0$$

$$\ddot{x}(0) = 12 \quad \dot{x}(0) = 5 \quad x(0) = 0.5$$

$$\ddot{x} + 4 \dot{x} + 10 x = 0$$

Step 1 :

$$\ddot{x}_m \frac{\ddot{x}}{\ddot{x}_m} + 4 \dot{x}_m \frac{\dot{x}}{\dot{x}_m} + 10 x_m \frac{x}{x_m} = 0$$

$$\ddot{x}_m \approx 4 \dot{x}_m \approx 10 x_m$$

$$x_m = 1 \quad \dot{x}_m = 2.5 \quad \ddot{x}_m = 10$$

Step 2:

Normalise the initial condition

$$\frac{\ddot{x}(0)}{\ddot{x}_m} = \frac{12}{10} > 1, \quad \frac{\dot{x}(0)}{\dot{x}_m} = 0, \quad \frac{x(0)}{x_m} = 0.5$$

Change  $\ddot{x}_m$  to make this normalised value less than or equal to 1

Step 3:

Arrange the maximum values increasing the  $\ddot{x}_m$  to 12.

$$x_m = 1 \quad \dot{x}_m = 2.5 \quad \ddot{x}_m = 12$$

Step 4 :

Put the numerical values of maximum to the normalized equation in step 1

$$12 \frac{\ddot{x}}{12} + 2(2.5) \frac{\dot{x}}{2.5} + 10 \times 1 \times \frac{x}{1} = 0$$

$$\frac{\ddot{x}(0)}{12} = \frac{12}{12} = 1 \quad \frac{\dot{x}(0)}{2.5} = \frac{0}{2.5} = 0 \quad \frac{x(0)}{1} = \frac{0.5}{1} = 0.5$$

There is other approach to the scaling problem apart from these classic ways. This approach is explained by Auslender(18). In this method, equations are written in state - variable format. Coefficient matrix is rearranged providing with scaling constant for time and state variables. All the coefficients are required to be as close to one as possible. The diagonal terms of rearranged matrix are the inversed time scale factor and characteristics terms of dynamic system. So

scaling starts by selection of  $kt$  and then diagonal terms are required straddle unity as evenly as possible. An important feature of this method is that no assumptions have yet been made concerning maximum values of any of the variables, or the type of computing equipment to be used.

The matrix of inputs is also re-arranged on the basis of the known maximum values of the inputs, scaling constants of time and state variables. The ratios of maximum values of inputs and state variables are chosen to obtain the values of terms as close to one as possible. So the state variable scaling coefficients should then be checked to make sure that none of the initial conditions causes an overload. In the mean time if there is some a priori knowledge of maximum values, this knowledge can be used to good advantage. This method is used to check the verification of time and magnitude scaling in this study. This scaling method is illustrated with following example.

Example 2 :

A linear system equations are given in state vector form. And the coefficients of state variables are given in matrix form.

$$\frac{dx}{dt} = Ax + BU$$

where

$$A = \begin{vmatrix} -500 & 20000 \\ -300 & -600 \end{vmatrix} \quad B = \begin{vmatrix} 0 \\ 1 \end{vmatrix}$$

Now two new matrices are defined for scaling. These contain all the scaling constants.



$$A^* = \begin{vmatrix} -K_t \cdot 500 & K_t \cdot 20000 \left( \frac{K_2}{K_1} \right) \\ -K_t \cdot 300 \left( \frac{K_1}{K_2} \right) & -K_1 \cdot 600 \end{vmatrix}$$

$$B^* = \begin{vmatrix} 0 \\ K_t \cdot 1 \cdot \frac{K_{ul}}{K_2} \end{vmatrix}$$

Where  $K_t$  is the inverse of time scaling constant  $K_1$  and  $K_2$  are the maximums of variables and  $K_{ul}$  is the maximum of input variable .

Now try to put the diagonal elements in the 0.1 - 10 range.

If  $K_t$  is chosen as 0,001, the diagonal elements fall in this range.

$$A^* = \begin{vmatrix} -0.5 & 20 \frac{K_2}{K_1} \\ -0.3 \frac{K_1}{K_2} & -0.6 \end{vmatrix}$$

If  $\frac{K_2}{K_1} = 0.2$ . then all of the elements fall in to the 0.1 and 1 range.

$$A^* = \begin{vmatrix} -0.5 & 4 \\ -11.5 & -0.6 \end{vmatrix}$$

$B^*$  is also determined in the same way

$$B^* = \begin{vmatrix} 0 \\ 0.001 \left( \frac{K_{ul}}{K_2} \right) \end{vmatrix}$$

where, if  $\frac{K_{ul}}{K_2} = 1000$

$$B^* = \begin{vmatrix} 0 \\ 1 \end{vmatrix}$$

At this point, the maximum values of any of the variables or the computer voltage range are required. If  $u_{max} = 2000$  and reference voltage of computer is 10, then

$$\frac{2000}{K_{ul}} = 10 \quad \text{and} \quad K_{ul} = 200$$

So  $K_2 = 0.2$  and  $K_1 = 1$ . The scaling is now complete.

If the set of the scaling constants does not fall into the 0.1 to 1.0 range, this generally means that the problem has been poorly formulated and it means that some parts of model respond very rapidly while the others have very slowly response character.

#### 4.5 SCALED EQUATIONS AND BLOCK DIAGRAM FOR THE FEED DRIVE MODEL

In this section, scaled equations and the block diagrams of the five and two inertia models are given. These are done on the basis of the section 3.4.

The equation 3.16 is expressed for the scaled equation as follows:

$$\ddot{\theta}_m = \frac{1}{n} \frac{D}{J} \frac{\dot{\theta}_m}{\dot{\theta}_m} + \frac{1}{n^2} \frac{K}{J} \frac{\theta_m}{\theta_m} + \frac{1}{n^2} \frac{T}{J} \frac{1}{\theta_m} \dots \dots \quad (4.3)$$

and coefficient matrices are given as follows :

$$\begin{array}{cccccc} \frac{(D_m + C_{Tc})}{J_1} \frac{\dot{\theta}_{1m}}{\dot{\theta}_{1m}} & \frac{C_{Tc}}{J_1} \frac{\dot{\theta}_{2m}}{\dot{\theta}_{1m}} & 0 & 0 & 0 & 0 \\ \frac{C_{Tc}}{J_2} \frac{\dot{\theta}_{1m}}{\dot{\theta}_{2m}} & -\frac{(C_{Tc} + D_{bd} + C_{s1})}{J_2} \frac{\dot{\theta}_{2m}}{\dot{\theta}_{2m}} & \frac{C_{s1}}{J_2} \frac{\dot{\theta}_{3m}}{\dot{\theta}_{2m}} & 0 & 0 & 0 \\ 0 & \frac{C_{s1}}{J_3} \frac{\dot{\theta}_{2m}}{\dot{\theta}_{3m}} & -\frac{(C_{s1} + C_{s2} + C_{nsT})}{J_3} \frac{\dot{\theta}_{3m}}{\dot{\theta}_{3m}} & \frac{C_{s2}}{J_3} \frac{\dot{\theta}_{4m}}{\dot{\theta}_{3m}} & \frac{C_{nsT}}{J_3} \frac{\dot{\theta}_{5m}}{\dot{\theta}_{3m}} & 0 \\ 0 & 0 & \frac{C_{s2}}{J_4} \frac{\dot{\theta}_{3m}}{\dot{\theta}_{4m}} & -\frac{C_{s2} + D_{ba}}{J_4} \frac{\dot{\theta}_{4m}}{\dot{\theta}_{4m}} & 0 & 0 \\ 0 & 0 & \frac{C_{nsT}}{J_5} \frac{\dot{\theta}_{3m}}{\dot{\theta}_{5m}} & 0 & 0 & \frac{(C_{nsT} + D_{tt})}{J_5} \frac{\dot{\theta}_{5m}}{\dot{\theta}_{5m}} \end{array} \quad (4.4)$$

$$\frac{n}{n} = \frac{1}{n^2} \left| \begin{array}{cccccc} -\frac{K_{Tc}}{J_1} \frac{\theta_{1m}}{\dot{\theta}_{1m}} & \frac{K_{Tc}}{J_1} \frac{\theta_{2m}}{\dot{\theta}_{1m}} & 0 & 0 & 0 & 0 \\ \frac{K_{Tc}}{J_2} \frac{\theta_{1m}}{\dot{\theta}_{2m}} & -\frac{(K_{Tc}+K_{Ts1})}{J_2} \frac{\theta_{2m}}{\dot{\theta}_{2m}} & \frac{K_{Ts1}}{J_2} \frac{\theta_{3m}}{\dot{\theta}_{2m}} & 0 & 0 & 0 \\ 0 & \frac{K_{Ts1}}{J_3} \frac{\theta_{2m}}{\dot{\theta}_{3m}} & -\frac{(K_{Ts1}+K_{Ts2}+K_{eaT})}{J_3} \frac{\theta_{3m}}{\dot{\theta}_{3m}} & \frac{K_{Ts2}}{J_3} \frac{\theta_{4m}}{\dot{\theta}_{3m}} & \frac{K_{eaT}}{J_3} \frac{\theta_{5m}}{\dot{\theta}_{3m}} & 0 \\ 0 & 0 & \frac{K_{Ts2}}{J_4} \frac{\theta_{3m}}{\dot{\theta}_{4m}} & -\frac{K_{Ts2}}{J_4} \frac{\theta_{4m}}{\dot{\theta}_{4m}} & 0 & 0 \\ 0 & 0 & \frac{K_{eaT}}{J_5} \frac{\theta_{3m}}{\dot{\theta}_{5m}} & 0 & -\frac{K_{eaT}}{J_5} \frac{\theta_{5m}}{\dot{\theta}_{5m}} & 0 \end{array} \right|$$

(4.5)

$$\frac{T}{J \ddot{\theta}_m} = \frac{1}{n^2} \left| \begin{array}{c} \frac{T}{J_1} \frac{1}{\dot{\theta}_{1m}} \\ 0 \\ 0 \\ 0 \\ 0 \end{array} \right|$$

(4.6)

In the same way, the coefficient matrices of the two inertia model are obtained as follows :

$$\frac{D \dot{\theta}_m}{n J \ddot{\theta}_m} = \frac{1}{n} \left| \begin{array}{cc} -\left( \frac{D+C}{J_1} \frac{nsT}{nsT} \right) \frac{\dot{\theta}_{1m}}{\dot{\theta}_{1m}} & \frac{C}{J_1} \frac{nsT}{nsT} \frac{\dot{\theta}_{2m}}{\dot{\theta}_{1m}} \\ \frac{C}{J_2} \frac{nsT}{nsT} \frac{\dot{\theta}_{1m}}{\dot{\theta}_{2m}} & -\left( \frac{D+C}{J_2} \frac{nsT}{nsT} \right) \frac{\dot{\theta}_{2m}}{\dot{\theta}_{2m}} \end{array} \right|$$

(4.7)

$$\frac{K \theta_m}{J \ddot{\theta}_m} = \frac{1}{n^2} \left| \begin{array}{cc} -\frac{K_{eaT}}{J_1} \frac{\theta_{1m}}{\dot{\theta}_{1m}} & \frac{K_{eaT}}{J_1} \frac{\theta_{2m}}{\dot{\theta}_{1m}} \\ \frac{K_{eaT}}{J_2} \frac{\theta_{1m}}{\dot{\theta}_{2m}} & -\frac{K_{eaT}}{J_2} \frac{\theta_{2m}}{\dot{\theta}_{2m}} \end{array} \right|$$

(4.8)

$$\frac{T}{J \ddot{\theta}_m} = \frac{1}{n^2} \left| \begin{array}{c} \frac{T}{J_1} \frac{1}{\dot{\theta}_{1m}} \\ 0 \end{array} \right|$$

(4.9)

Scaled loop equations and d.c. motor equations are given in equations 4.10 - 4.14

$$B = A - \theta_{2m} \left( \frac{\theta_2}{\theta_{2m}} \right) \quad (4.10)$$

$$C = BK_p - n \dot{\theta}_{1m} \left( \frac{\dot{\theta}_1}{\dot{\theta}_{1m}} \right) \quad (4.11)$$

$$V = C \cdot K_v \quad (4.12)$$

$$\frac{I}{I_m} = \int_0^{\tau} \left( \frac{V}{n \cdot L I_m} - \frac{R}{nL} \frac{I}{I_m} - \frac{K_B \cdot \dot{\theta}_{1m}}{L \cdot I_m} \frac{\dot{\theta}_1}{\dot{\theta}_{1m}} \right) d\tau \quad (4.13)$$

$$T_g = K_T \cdot I_m \frac{I}{I_m} \quad (4.14)$$

The analog computer diagrams are drawn according to these equation. Analog computer diagrams of five inertia model and two inertia model are illustrated in figures 4.5 and 4.6.

The inductance of dc motor has a very small value. Therefore, the equation 3.5 are replaced by 4.15 and the scaled form of this equation, 4.13, are replaced by 4.16. These are given as follows :

$$I = \frac{V - K_B \cdot \dot{\theta}_1}{R} \quad (4.15)$$

$$\frac{I}{I_m} = \frac{V}{R_{Im}} - \frac{n K_B \dot{\theta}_{1m}}{R I_m} \left( \frac{\dot{\theta}_1}{\dot{\theta}_{1m}} \right) \quad (4.16)$$

The analog computer diagram of two inertia model without motor inductances is shown in figure 4.7.

The scaled coefficient matrices of non - linear two inertia model are written as follows :

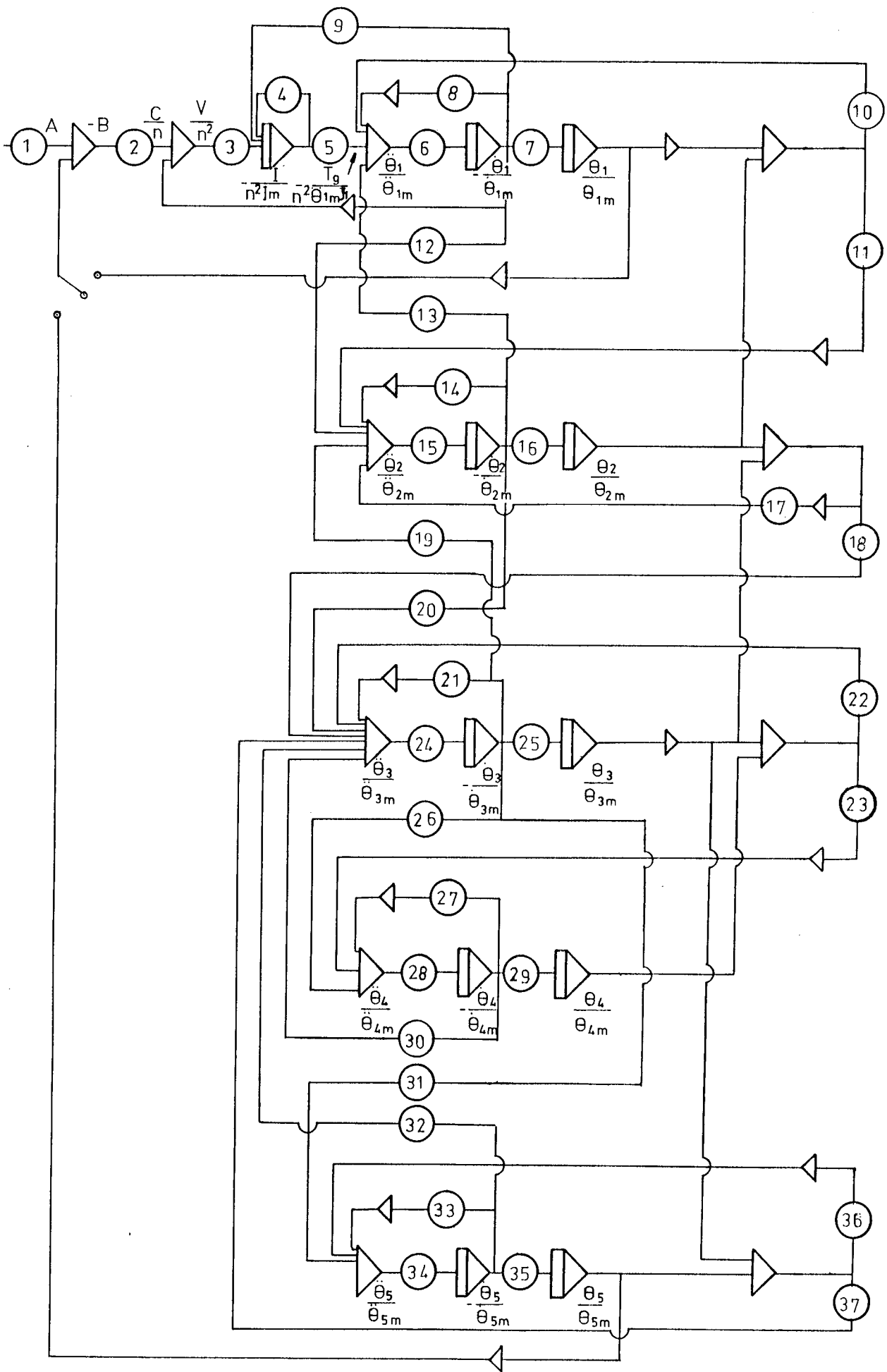
$$\frac{D\dot{\theta}_m}{nJ\ddot{\theta}_m} = \frac{1}{n} \left| \begin{array}{cc} - \frac{D+C}{J_1} \frac{\dot{\theta}_{1m}}{\dot{\theta}_{1m}} & \frac{C}{J_1} \frac{\dot{\theta}_{2m}}{\dot{\theta}_{1m}} \\ \frac{C}{J_2} \frac{\dot{\theta}_{1m}}{\dot{\theta}_{2m}} & - \frac{C+D}{J_2} \frac{\dot{\theta}_{2m}}{\dot{\theta}_{2m}} \end{array} \right| \quad (4.17)$$

$$\frac{K\theta_m}{n^2J\ddot{\theta}_m} = \frac{1}{n^2} \left| \begin{array}{cc} - \frac{K}{J_1} \frac{\theta_{1m}}{\theta_{1m}} & \frac{K}{J_1} \frac{\theta_{2m}}{\theta_{1m}} \\ \frac{K}{J_2} \frac{\theta_{1m}}{\theta_{2m}} & - \frac{K}{J_2} \frac{\theta_{2m}}{\theta_{2m}} \end{array} \right| \quad (4.18)$$

$$\frac{T}{n^2J\ddot{\theta}_m} = \frac{1}{n^2} \left| \begin{array}{cc} \frac{T}{J_1} \frac{\theta_{1m}}{\theta_{1m}} & - \text{Sign } \dot{\theta}_1 \frac{T_{fm}}{J_1 \dot{\theta}_{1m}} \\ 0 & - \text{Sign } \dot{\theta}_2 \frac{T_{fs}}{J_2 \ddot{\theta}_{2m}} \end{array} \right| \quad (4.19)$$

The analog computer diagram of two inertia non-linear model without motor inductance effect is illustrated in figure 4.8.

While the analog computer diagram is constructed, the maximum values of all positions are assumed as equal to each other. According to the relevant figures, the symbolic representation of potentiometers in the analog computer diagrams of two and five inertia models are given in tables 4.1, 4.2, 4.3. and 4.4.



4.5. Analog Computer Diagram for Five-Inertia Linear Model (L)

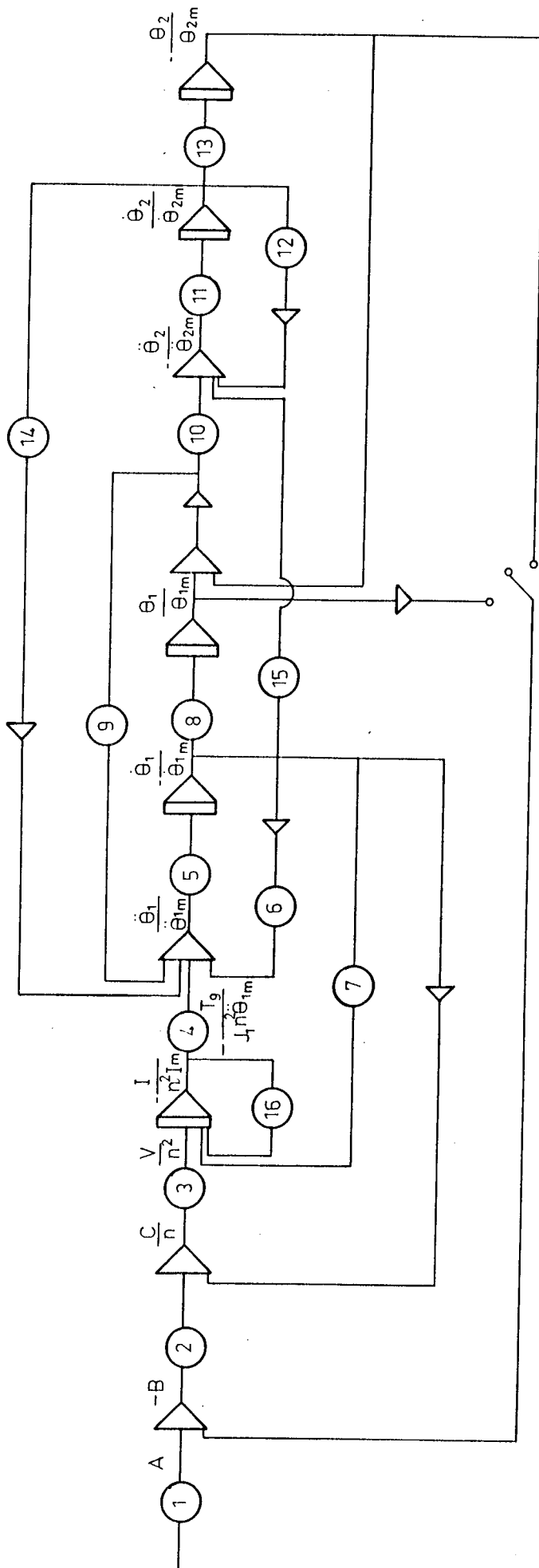


Fig. 4.6 Analog Computer Diagram for Two - Inertia Linear Model ( L )

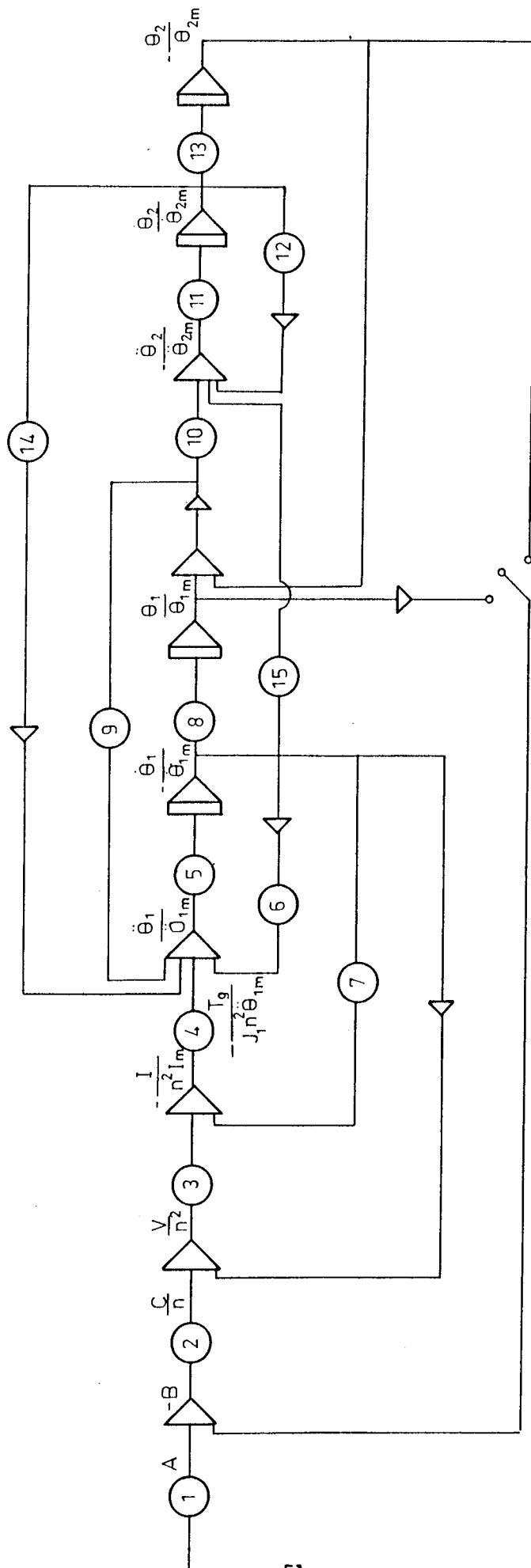


Fig. 4.7 Analog Computer Diagram for Two-Inertia Linear Model ( $L=0$ )



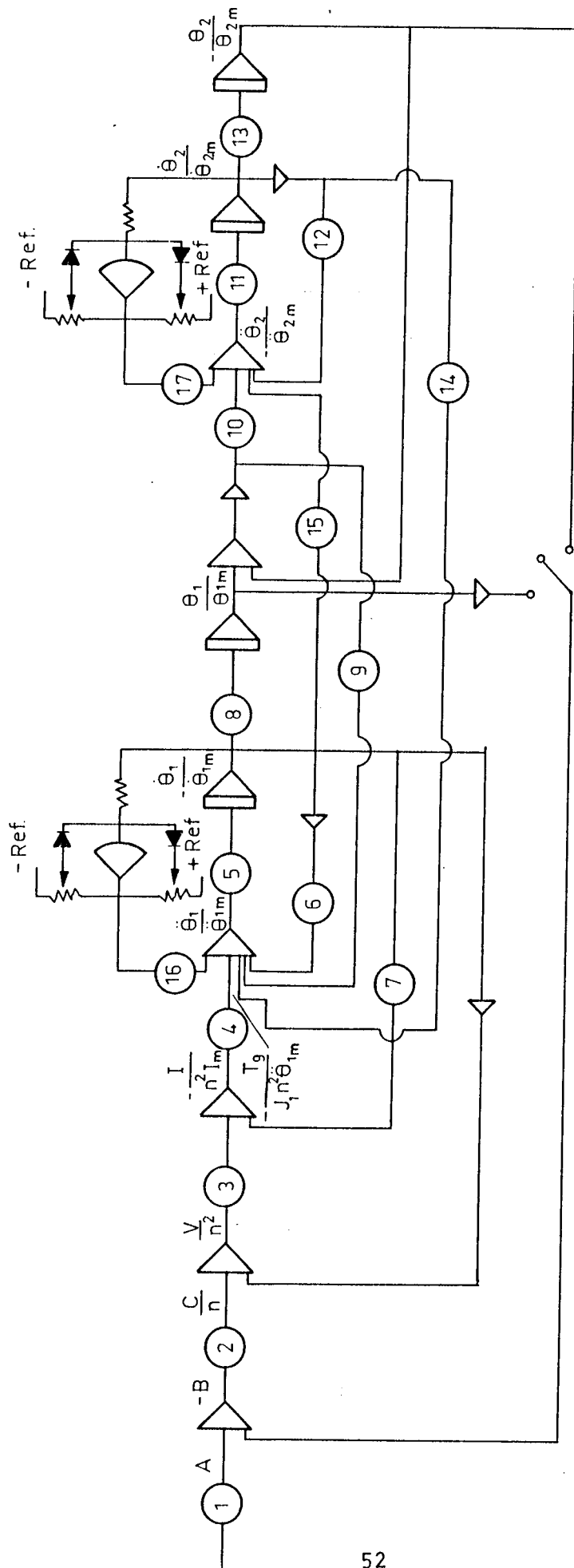


Fig. 4.8 Analog Computer Diagram for Two-Inertia Non-Linear Model.

Table 4.1 Symbolic Representation of Potentiometers For Figure 4.5

Pot No	Sym. Rep.	Pot No	Sym. Rep.	Pot No	Sym. Rep.
1	$\frac{1}{K_E \cdot \theta_{1m}}$	14	$\frac{(C_{Tc} + D_{bd} + C_{s1}) \ddot{\theta}_{2m}}{n \cdot J_2 \cdot \ddot{\theta}_{2m}}$	26	$\frac{C_{s2} \cdot \dot{\theta}_{3m}}{n \cdot J_4 \cdot \ddot{\theta}_{4m}}$
2	$\frac{K_P \cdot \theta_{1m}}{n \cdot \dot{\theta}_{1m}}$	15	$\frac{\ddot{\theta}_{2m}}{\dot{\theta}_{2m}}$	27	$\frac{(C_{s2} + D_{bd}) \cdot \dot{\theta}_{4m}}{n \cdot J_4 \cdot \ddot{\theta}_{4m}}$
3	$\frac{K_V \cdot \dot{\theta}_{1m}}{n^2 \cdot L \cdot I_m}$	16	$\frac{\dot{\theta}_{2m}}{\theta_{2m}}$	28	$\frac{\ddot{\theta}_{4m}}{\dot{\theta}_{4m}}$
4	$\frac{R}{n^3 \cdot L}$	17	$\frac{K_{Ts1} \cdot \theta_{2m}}{n^2 \cdot J_2 \cdot \ddot{\theta}_{2m}}$	29	$\frac{\dot{\theta}_{4m}}{\theta_{4m}}$
5	$\frac{K_T \cdot I_m}{J_1 \cdot \ddot{\theta}_{1m}}$	18	$\frac{K_{Ts1} \cdot \theta_{3m}}{n^2 \cdot J_3 \cdot \ddot{\theta}_{3m}}$	30	$\frac{C_{s2} \cdot \dot{\theta}_{4m}}{n \cdot J_3 \cdot \ddot{\theta}_{3m}}$
6	$\frac{\ddot{\theta}_{1m}}{\dot{\theta}_{1m}}$	19	$\frac{C_{s1} \cdot \dot{\theta}_{3m}}{n \cdot J_2 \cdot \ddot{\theta}_{2m}}$	31	$\frac{C_{nsT} \cdot \dot{\theta}_{3m}}{n \cdot J_5 \cdot \ddot{\theta}_{5m}}$
7	$\frac{\dot{\theta}_{1m}}{\theta_{1m}}$	20	$\frac{C_{s1} \cdot \dot{\theta}_{3m}}{n \cdot J_3 \cdot \ddot{\theta}_{3m}}$	32	$\frac{C_{nsT} \cdot \dot{\theta}_{5m}}{n \cdot J_5 \cdot \ddot{\theta}_{5m}}$
8	$\frac{(C_{Tc} + D_m) \cdot \dot{\theta}_{1m}}{n \cdot J_1 \cdot \ddot{\theta}_{1m}}$	21	$\frac{(C_{s1} + C_{s2} + C_{nsT}) \cdot \dot{\theta}_{3m}}{n \cdot J_3 \cdot \ddot{\theta}_{3m}}$	33	$\frac{(C_{nsT} + D_{tT}) \cdot \dot{\theta}_{5m}}{n \cdot J_5 \cdot \ddot{\theta}_{5m}}$
9	$\frac{K_B \cdot \dot{\theta}_{1m}}{n^2 \cdot L \cdot I_m}$	22	$\frac{K_{Ts2} \cdot \theta_{3m}}{n^2 \cdot J_3 \cdot \ddot{\theta}_{3m}}$	34	$\frac{\ddot{\theta}_{5m}}{\dot{\theta}_{5m}}$
10	$\frac{K_{Tc} \cdot \theta_{1m}}{n^2 \cdot J_1 \cdot \ddot{\theta}_{1m}}$	23	$\frac{K_{Ts2} \cdot \theta_{4m}}{n^2 \cdot J_4 \cdot \ddot{\theta}_{4m}}$	35	$\frac{\dot{\theta}_{5m}}{\theta_{5m}}$
11	$\frac{K_{Tc} \cdot \theta_{2m}}{n^2 \cdot J_2 \cdot \ddot{\theta}_{2m}}$	24	$\frac{\ddot{\theta}_{3m}}{\dot{\theta}_{3m}}$	36	$\frac{K_{eaT} \cdot \theta_{5m}}{n^2 \cdot J_5 \cdot \ddot{\theta}_{5m}}$
12	$\frac{C_{Tc} \cdot \dot{\theta}_{1m}}{n \cdot J_2 \cdot \ddot{\theta}_{2m}}$	25	$\frac{\dot{\theta}_{3m}}{\theta_{3m}}$	37	$\frac{K_{eaT} \cdot \theta_{3m}}{n^2 \cdot J_3 \cdot \ddot{\theta}_{3m}}$
13	$\frac{C_{Tc} \cdot \dot{\theta}_{2m}}{n \cdot J_1 \cdot \ddot{\theta}_{1m}}$				

Table 4.2 Symbolic Representation of Potentiometers For Figure 4.6

Pot No	Sym Rep.	Pot No	Sym Rep.
1	$\frac{1}{K_E \cdot \theta_{1m}}$	9	$\frac{K_{eaT} \theta_{1m}}{n^2 J_1 \ddot{\theta}_{1m}}$
2	$\frac{K_p \cdot \theta_{1m}}{n \cdot \dot{\theta}_{1m}}$	10	$\frac{K_{eaT} \cdot \theta_{2m}}{n^2 J_2 \ddot{\theta}_{2m}}$
3	$\frac{K_v \cdot \dot{\theta}_{1m}}{n^2 \cdot L \cdot I_m}$	11	$\frac{\ddot{\theta}_{2m}}{\dot{\theta}_{2m}}$
4	$\frac{K_T I_m}{J_1 \ddot{\theta}_{1m}}$	12	$\frac{D_{tT} \dot{\theta}_{2m}}{n \cdot J_2 \ddot{\theta}_{2m}}$
5	$\frac{\ddot{\theta}_{1m}}{\dot{\theta}_{1m}}$	13	$\frac{\dot{\theta}_{2m}}{\theta_{2m}}$
6	$\frac{D_m \dot{\theta}_{1m}}{n \cdot J_1 \ddot{\theta}_{1m}}$	14	$\frac{C_{nsT} \dot{\theta}_{2m}}{n \cdot J_1 \ddot{\theta}_{1m}}$
7	$\frac{K_B \dot{\theta}_{1m}}{n \cdot L \cdot I_m}$	15	$\frac{C_{nsT} \dot{\theta}_{2m}}{n \cdot J_1 \ddot{\theta}_{2m}}$
8	$\frac{\dot{\theta}_{1m}}{\theta_{1m}}$	16	$\frac{R}{n^3 \cdot L}$

Table 4.3 Symbolic Representation of Potentiometers For Figure 4.7

Pot No	Sym Rep.	Pot No	Sym Rep.
1	$\frac{1}{K_E \theta_{1m}}$	9	$\frac{K_{eat} \cdot \theta_{2m}}{n^2 J_1 \ddot{\theta}_{1m}}$
2	$\frac{K_p \cdot \theta_{1m}}{n \cdot \dot{\theta}_{1m}}$	10	$\frac{K_{eat} \cdot \theta_{1m}}{n^2 J_1 \ddot{\theta}_{1m}}$
3	$\frac{K_v \cdot \dot{\theta}_{1m}}{R \cdot n \cdot I_m}$	11	$\frac{\ddot{\theta}_{2m}}{\dot{\theta}_{2m}}$
4	$\frac{K_T I_m}{J_1 \ddot{\theta}_1}$	12	$\frac{D_{tT} \dot{\theta}_{2m}}{n J_2 \ddot{\theta}_{2m}}$
5	$\frac{\ddot{\theta}_{1m}}{\dot{\theta}_{1m}}$	13	$\frac{\dot{\theta}_{2m}}{\theta_{2m}}$
6	$\frac{D_m \dot{\theta}_{1m}}{n J_1 \ddot{\theta}_{1m}}$	14	$\frac{C_{nsT} \dot{\theta}_{2m}}{n J_1 \ddot{\theta}_{1m}}$
7	$\frac{K_B J \cdot \dot{\theta}_{1m}}{n R I_m}$	15	$\frac{C_{nsT} \cdot \dot{\theta}_{1m}}{n \cdot J_2 \cdot \ddot{\theta}_{2m}}$
8	$\frac{\dot{\theta}_{1m}}{\theta_{1m}}$		

Table 4.4 Symbolic Representation of Potentiometers For Figure 4.8

Pot No	Sym Rep.	Pot No	Sym Rep.
1	$\frac{1}{K_E \theta_{1m}}$	10	$\frac{K_{ed} \theta_{1m}}{n^2 J_1 \ddot{\theta}_{1m}}$
2	$\frac{K_p \theta_{1m}}{n \theta_{1m}}$	11	$\frac{\ddot{\theta}_{2m}}{\dot{\theta}_{2m}}$
3	$\frac{K_v \dot{\theta}_{1m}}{n^2 L I_m}$	12	$\frac{D_t \dot{\theta}_{2m}}{n J_2 \ddot{\theta}_{2m}}$
4	$\frac{K_T I_m}{J_1 \ddot{\theta}_{1m}}$	13	$\frac{\ddot{\theta}_{2m}}{\theta_{2m}}$
5	$\frac{\ddot{\theta}_{1m}}{\dot{\theta}_{1m}}$	14	$\frac{C_{nsT} \dot{\theta}_{2m}}{n J_2 \ddot{\theta}_{2m}}$
6	$\frac{(D_m + C_{nsT}) \dot{\theta}_{1m}}{n J_1 \ddot{\theta}_{1m}}$	15	$\frac{C_{nsT} \dot{\theta}_{1m}}{n J_2 \ddot{\theta}_{2m}}$
7	$\frac{K_B \dot{\theta}_{1m}}{n^2 L I_m}$	16	$\frac{T_{fm}}{n^2 J_1 \ddot{\theta}_{1m} \cdot 10}$
8	$\frac{\dot{\theta}_{1m}}{\theta_{1m}}$	17	$\frac{T_{fs}}{n^2 J_2 \ddot{\theta}_{2m} \cdot 10}$
9	$\frac{K_{edT} \theta_{2m}}{n^2 J_1 \ddot{\theta}_{1m}}$		

## CHAPTER 5

### EVALUATION OF DYNAMIC PERFORMANCE

#### 5.1 INTRODUCTION

The aim of this chapter is to illustrate the approach developed in this thesis on the evaluation of the dynamic performance of a feed drive system of a machine tool.

The set - up used in analog simulation is presented in section 5.2. In section 5.3, the effects of parameter variation on the dynamic performance is illustrated with a realistic example chosen from a machine tool available in the market.

#### 5.2 EXPERIMENTAL SET - UP

The experimental set - up consists of a readout equipment which is an oscilloscope and two analog computers as shown in figure 5.1.

Computers are a Comdyna product, GP-6 . Each one of these has 8 potentiometers, 4 integrators which can be used as summer or inverter, 2 summers which can be used as inverter, 2 inverters 2 multipliers. Reference voltage of the computer is 10 voltage. Computers can be used with both oscilloscope and X - Y plotter. If an oscilloscope is used as an readout equipment the repetitive operation is available, but if a X - Y recorder is used for this purpose then computer is operated with three available mode which are normal initial condition mode, hold operation mode and normal operate mode.

If the computer operates at repetitive operation, computer time is used to adjust the solution time but at the slow time operation, program time and computer time are the same. Repetitive operation operates 400

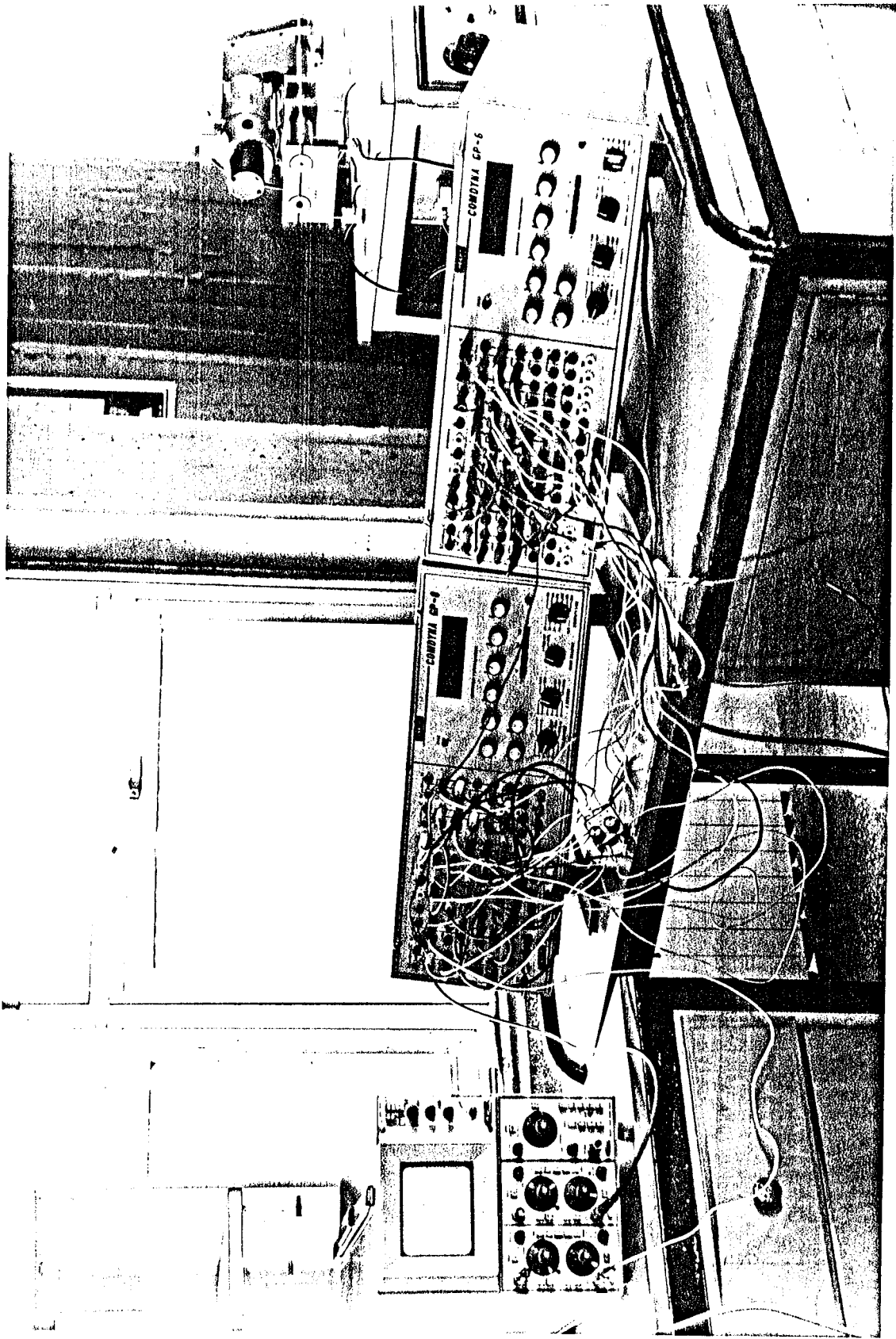


Fig.5.1 Experimental Set - up

time quicker than slow time operation.

The amplifiers of computer are connected to the readout equipment from rear terminal as y output for both computer and readout equipment. X output of computer is connected to the readout equipment as an absisa. The output of amplifier can be read with oscilloscope or digital voltmeter of computer. When the outputs exceed the reference voltage, an amplifier overload indicator which is a lamp operates so precautions are applied.

The capacity of the computers can be increased by slaving two computers. This can be done by removing the shorting connector of op output and op input at the rear terminal of the computer which is to slave and connecting the op output of the computer which is to be master to the op input terminal of the computer that is to be slave. The integrator mode control of the master will then control the integrators of the slave. In this study, computers are used as a single operating unit as explained above.

GP-6 can be used to solve linear, non-linear differential equations or partial differential equations and for transfer function simulation. Some non-linear function can be obtained using the limiter, dead space, diod, potentiometers and function switches.

An external logic level are compatible with the computer's mode control, integrators may be controlled by removing the shorting connector between op output to op input. In addition GP-6 can operate with a digital computer as a hybrid system.

The recording equipment is an oscilloscope of type Tektronix 5403.

### 5.3 ILLUSTRATIVE EXAMPLE

#### 5.3.1 Setting up the Example

The feed drive for the z-axis of a three axis nc lathe is chosen as an example. The configuration of the axis is given in figure 5.2. It is a direct drive which consists of a dc servomotor, a coupling,



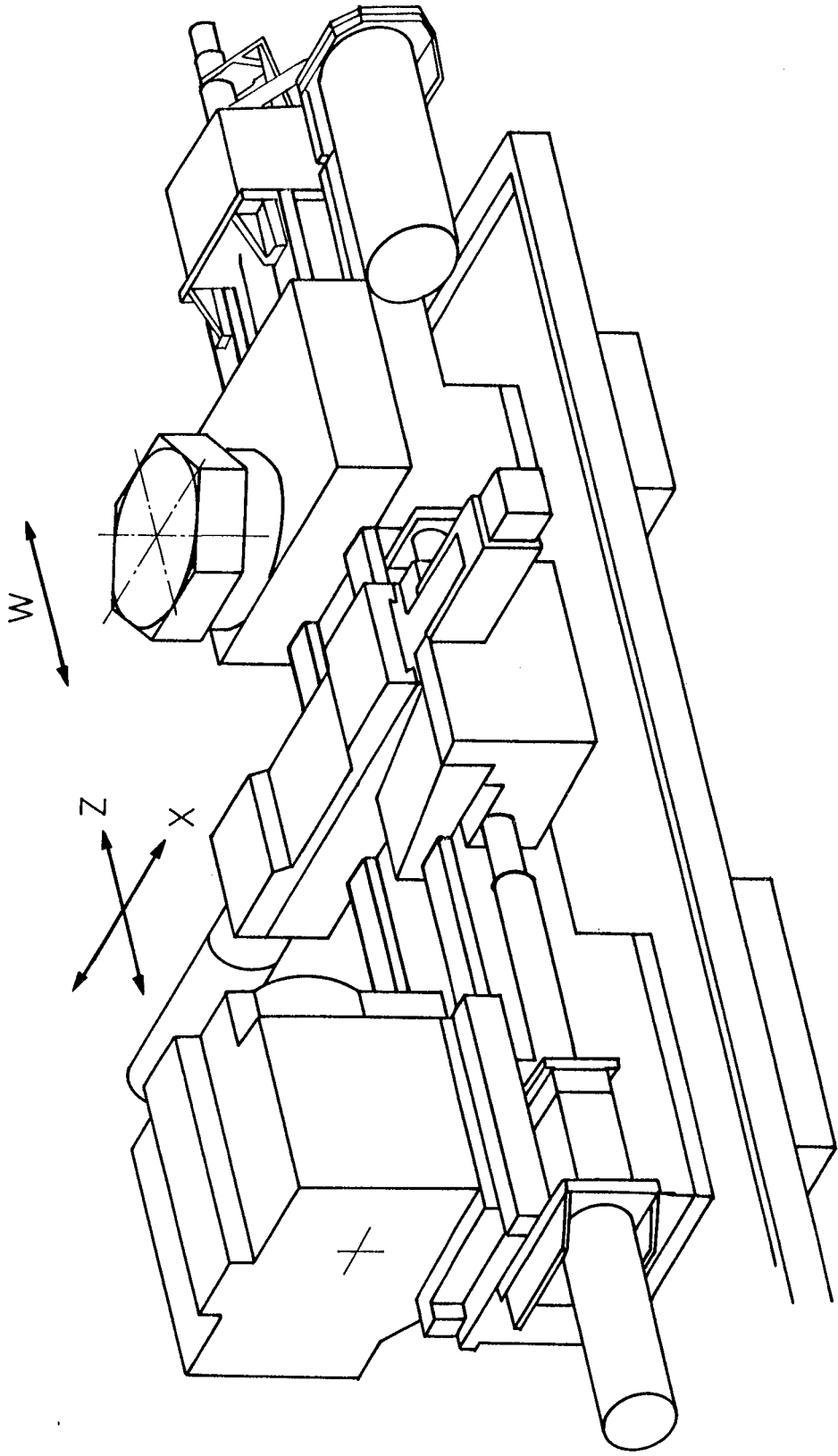


Fig 5.2 Layout of Feed Drive Axes

a ball - screw nut transmission and a plain slideway system. In this example, ball bearing screw assembly is of single ended type.

The inductance of dc motor and material damping coefficient of nut - screw assembly are neglected. The rest of the parameters specified in figure 3.19 are given in table 5.1 for this example. In addition all inertias of model components are given in table 5.2.

Table 5.1 Parameter Values

$K_{eaT} = 1136 \text{ Nm/rad}$	$K_B = 0.75 \text{ V/rad/sec}$
$J_1 = 0.02466 \text{ kg-m}^2$	$R = 0.56 \text{ ohm}$
$J_2 = 0.0006332 \text{ kg-m}^2$	$K_E = 796 \text{ Pulse/rad}$
$D_m = 0.0015 \text{ Nm/rad/sec}$	$K_p = 20$
$D_{tT} = 0.045 \text{ Nm/rad/sec}$	$K_V = 500$
$K_T = 0.75 \text{ Nm/amp}$	$P = 10 \text{ mm/rev}$
$\mu = 0.1$	

Table 5.2 Inertias of the Components

$J_m = 0.015 \text{ kg-m}^2$	$J_s = 0.5775 \times 10^{-2} \text{ kg-m}^2$
$J_{bd} = 0.00245 \text{ kg-m}^2$	$J_{ba} = 0.3617 \times 10^{-4} \text{ kg-m}^2$
$J_c = 0.0014 \text{ kg-m}^2$	$J_T = 0.0006332 \text{ kg-m}^2$

### 5.3.2 Analog Simulation

If table 5.1 is examined, it is seen that the natural frequency of system is considerably high. Therefore time scale factor is selected as 150. So the system is sufficiently slowed down. This selection is done according to the method explained in chapter 4 by taking the characteristics of this particular system into account.

The maximum values of the variables are estimated by using the method described in the previous chapter. For the results which will

be presented in the next section, maximum values of the variables are given in table 5.3

Table 5.3 Estimated Maximum Values

$\theta_{1m} = 0.1 \text{ rad}$	$\theta_{2m} = 0.1 \text{ rad}$
$\dot{\theta}_{1m} = 0.1 \text{ rad/sec}$	$\dot{\theta}_{2m} = 1,8 \text{ rad/sec}$
$\ddot{\theta}_{1m} = 1 \text{ rad/sec}^2$	$\ddot{\theta}_{2m} = 18 \text{ rad/sec}^2$
$I_m = 0.1 \text{ amp}$	

Potentiometer assignment referring to figures 5.3 and 5.4 are calculated by using these maximums and their values are given in table 5.4. The time scale factor and the maximums of the variables are verified by using the method which is described in section 4.4.3. In this study, friction at motor bearings is not included because of the limited capacity of the computers. Therefore the value of potentiometer 14 is assumed as zero. In addition while the analog computer diagrams are drawn,  $\theta_{1m}$  and  $\theta_{2m}$  are considered to be equal to each other. And diagrams are drawn based on this assumption.

Analog computer diagram is patched to the computer and potentiometers are set by using table 5.4.

The input to the system is of step type and the position responses of the motor and the table are given in Figure 5.5. To examine the changes in the responses to a parameter variation, it is assumed that all the rest of the parameters have their original values.

Equivalent axial stiffness, inertia of the table, damping coefficient of the table, friction between table and slideway, velocity and position loop gains are varied and the results due to these variations are given in the following

a) Influence of the equivalent Axial Stiffness

When the equivalent axial stiffness,  $K_{ea}$ , is increased, the effect of damping in the system reduces as shown in figure 5.8. In fact, if the stiffness is increased to a higher value, the system becomes

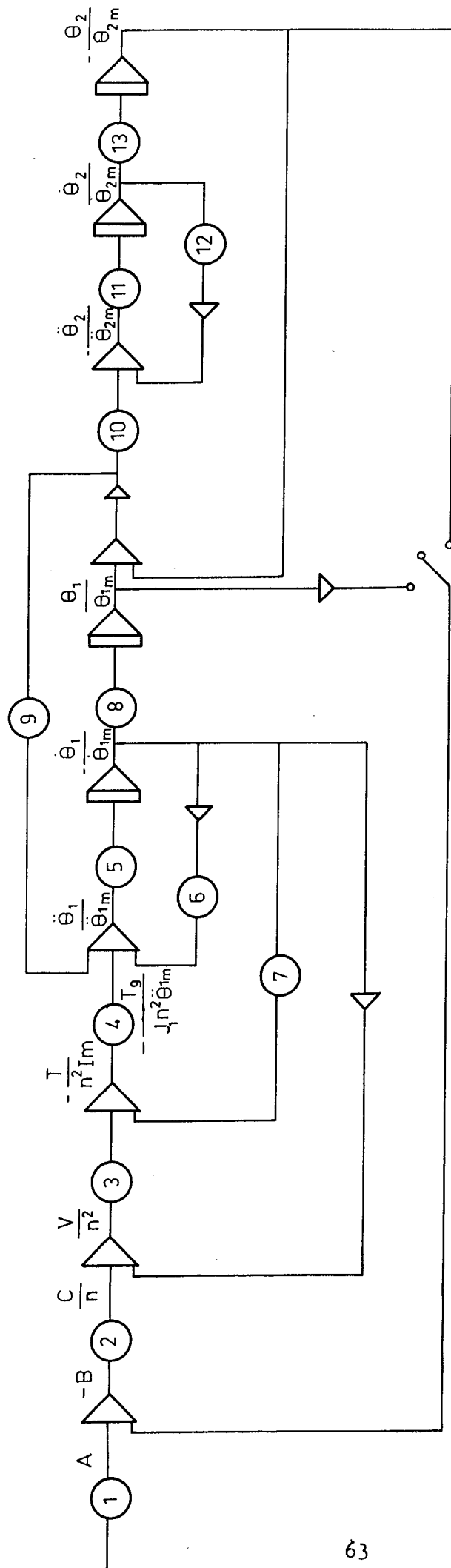


Fig. 5.3 Analog Computer Diagram for Two - Inertia Linear Model (L=0)

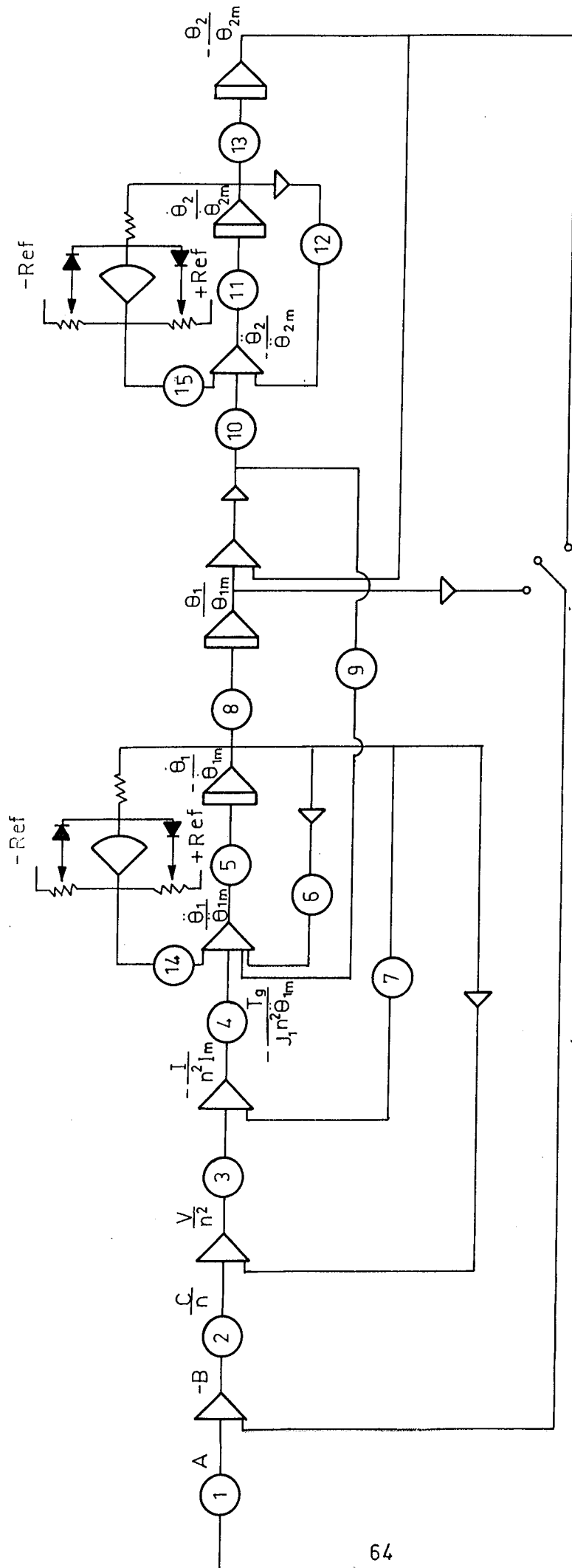


Fig. 5.4 Analog Computer Diagram for Two-Inertia Non-Linear Model ( $L=0$ )

Table 5.4 Values of the Potentiometers

Pot No	Sym Rep	Num. Values	Pot No	Sym Rep.	Num. Values
1	$\frac{1}{K_E \cdot \theta_{1m}}$	0.0125	9	$\frac{K_{edT} \theta_{2m}}{n^2 J_1 \dot{\theta}_{1m}}$	0.200
2	$\frac{K_p \theta_{1m}}{n \cdot \dot{\theta}_{1m}}$	0.133	10	$\frac{K_{edT} \theta_{1m}}{n^2 J_2 \ddot{\theta}_{2m}}$	0.45
3	$\frac{K_v \dot{\theta}_{1m}}{n R I_m}$	$0.59 \times 10$	11	$\frac{\ddot{\theta}_{2m}}{\dot{\theta}_{2m}}$	$1 \times 10$
4	$\frac{K_T I_m}{J_1 \ddot{\theta}_{1m}}$	$0.304 \times 10$	12	$\frac{D_{tT} \dot{\theta}_{2m}}{n J_2 \ddot{\theta}_{2m}}$	0.050
5	$\frac{\ddot{\theta}_{1m}}{\dot{\theta}_{1m}}$	$1 \times 10$	13	$\frac{\dot{\theta}_{2m}}{\theta_{2m}}$	$0.18 \times 100$
6	$\frac{D_m \dot{\theta}_{1m}}{n \cdot J_1 \ddot{\theta}_{1m}}$	$\sim 0$	14	$\frac{T_{fm} \text{ (Coulomb)}}{n^2 J_1 \ddot{\theta}_{1m}}$	0.0036
7	$\frac{K_B \dot{\theta}_{1m}}{n R I_m}$	0.010	15	$\frac{T_{fs} \text{ (Coulomb)}}{n^2 J_2 \ddot{\theta}_{2m}}$	0.0183
8	$\frac{\dot{\theta}_{1m}}{\theta_{1m}}$	1			

unstable as shown in figures 5.6 and 5.7.

While equivalent axial stiffness is reduced to a definite value the positioning accuracy is still kept in spite of roughness of motion (see figure 5.9). But the accuracy of positioning and the smoothness of motion are reduced at very low stiffness values as shown in figures 5.10 and 5.11.

b) Influence of the Inertia of the Slide

If the slide inertia is increased, the smoothness of the motion and the positioning accuracy are reduced as shown in figures 5.13 and 5.14. If the slide inertia is increased to a  $3J_2$ , the positioning of table will become impossible because of limit cycle which is not required (see figure 5.12).

But while the slide inertia of table is decreased, it does not exert any influence on the performance of the system (see figures 5.15 and 5.16) because the capacity of actuator is enough to move the table and tooling.

c) Influence of Damping Coefficient

When the damping coefficient is increased, more uniform motion is obtained as shown in figures 5.17 - 5.19. But when it is reduced to lower values the system becomes unstable and positioning will be impossible as illustrated in figures 5.20 and 5.21.

d) Influence of Position and Velocity loop gains.

The multiplication of position loop gain,  $K_p$ , and velocity loop gain,  $K_v$ , must be higher than deadband to overcome the frictional torques in feed drive components when the minimum motion is called for. Because of this, the product of  $K_p$  and  $K_v$  is held as constant. So the  $K_p$  and  $K_v$  are varied depending on this constraint.

According to the above explanations, when the position loop gain is decreased and velocity loop gain is increased proportionally, a soft servo system is obtained. As a result of this, the system slows down and if  $K_p$  is reduced and  $K_v$  is increased by 4 then system does not reach its steady state value (see figures 5.22 - 5.24).

If  $K_p$  is increased and  $K_v$  is decreased proportionally, a hard servo is obtained. In this case, system becomes very fast (see figures 5.25 and 5.26). If  $K_p$  is increased to much higher values then overshoot can be seen. Figure 5.27 represents the transient of this phenomena.

e) Influence of the Friction

The friction torque at table adversely effects the smoothness of motion and positioning accuracy and the steady state value of motor shaft position decreases from this reason. These cases are illustrated in figure 5.28 - 5.30.

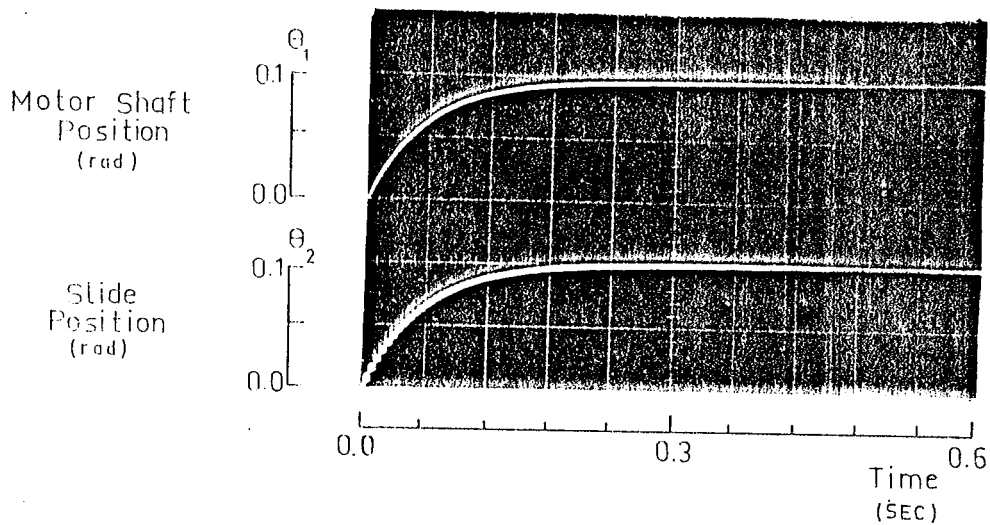


Fig 5.5 System Response at Original Parameter Values.



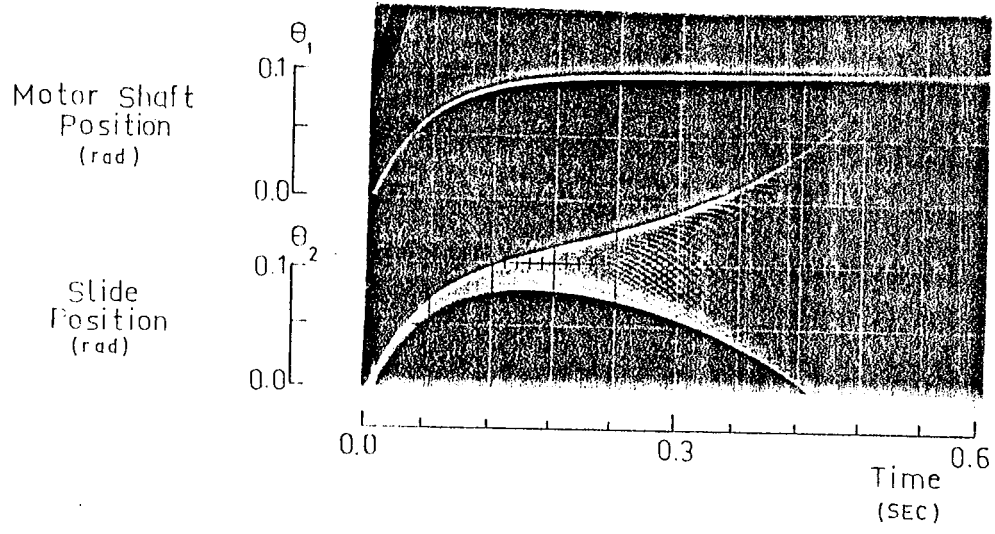


Fig. 5.6 Effect of  $K_{eaT}$  ( $K_{eaT}^* = 4K_{eaT}$ )

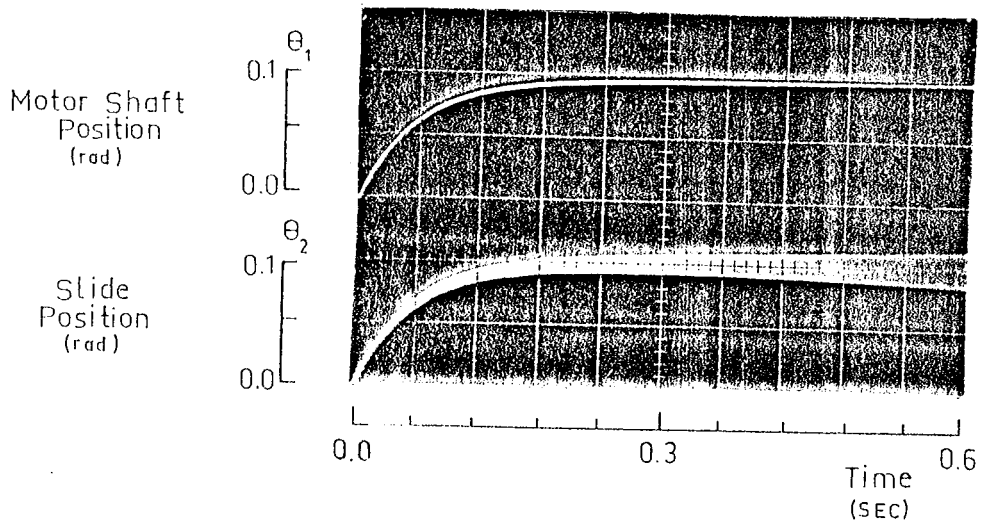


Fig. 5.7. Effect of  $K_{eaT}$  ( $K_{eaT}^* = 3K_{eaT}$ )

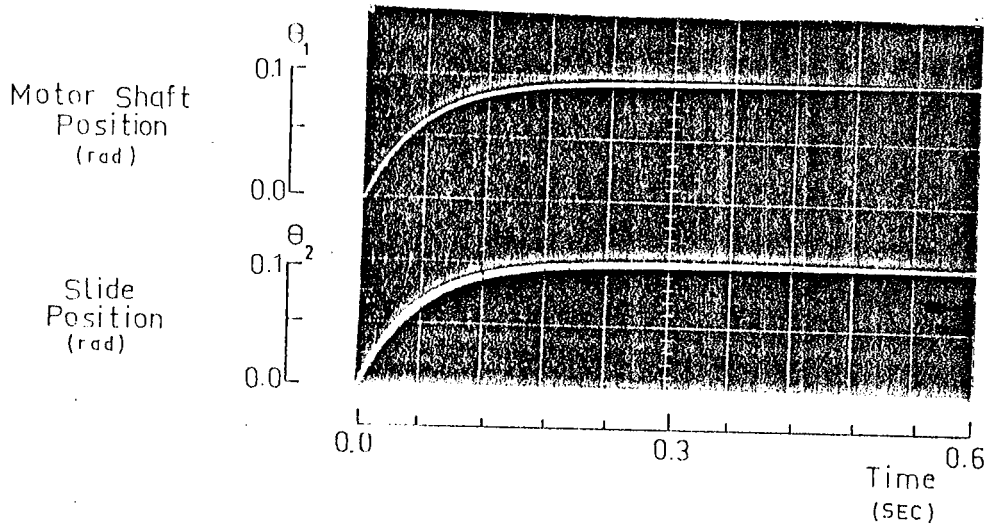


Fig. 5.8 Effect of  $K_{edT}^* (K_{edT}^* = 2 K_{edT})$

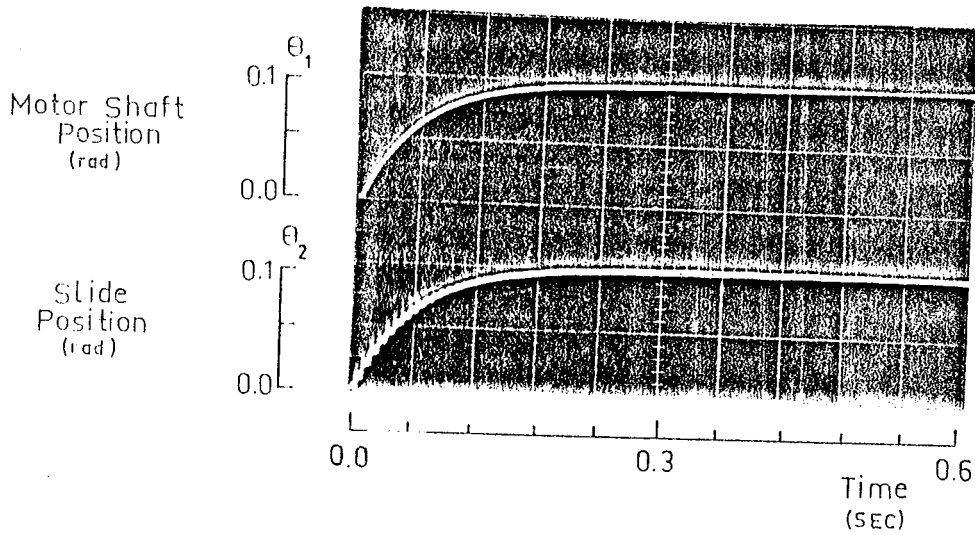


Fig 5.9 Effect of  $K_{edT} (K_{edT}^* = \frac{1}{2} K_{edT})$

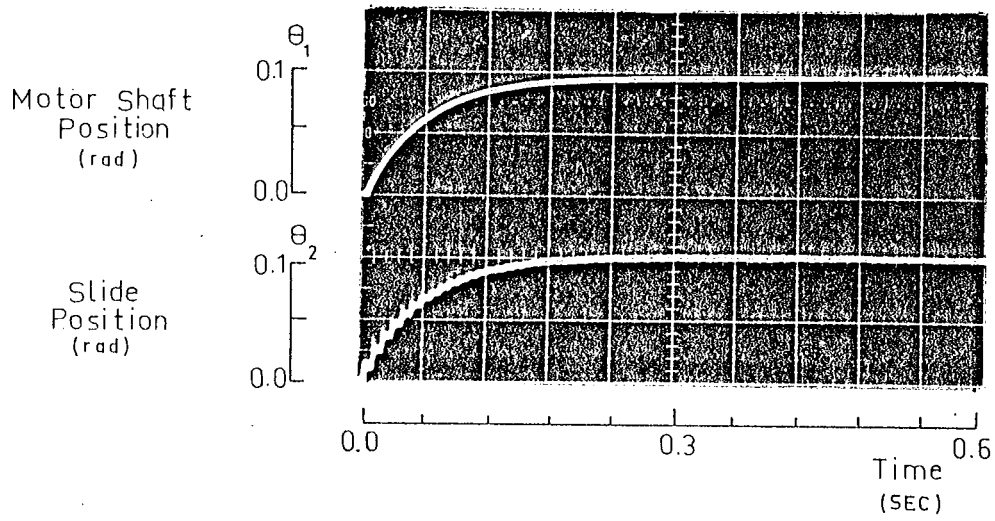


Fig .5.10 Effect of the  $K_{edT}$  ( $K_{edT}^* = \frac{1}{3} K_{edT}$ )

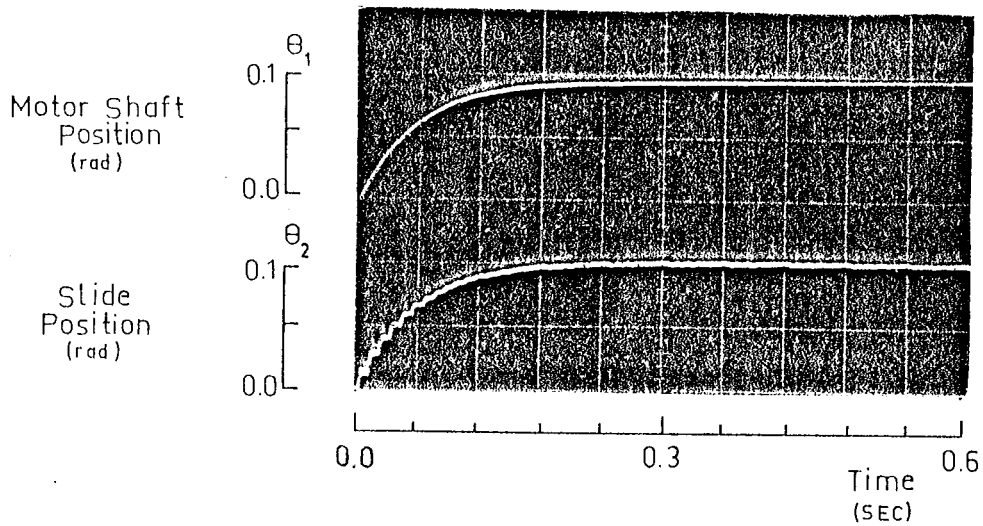


Fig .5.11 Effect of the  $K_{edT}$  ( $K_{edT}^* = \frac{1}{4} K_{edT}$ )

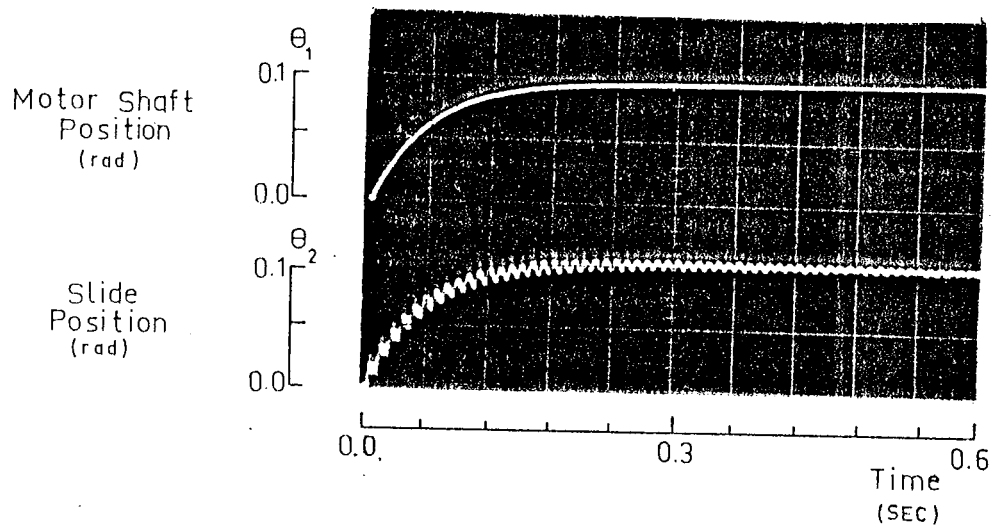


Fig. 5.12 Effect of the Equivalent Slide Inertia ( $J_2^* = 4 J_2$ )

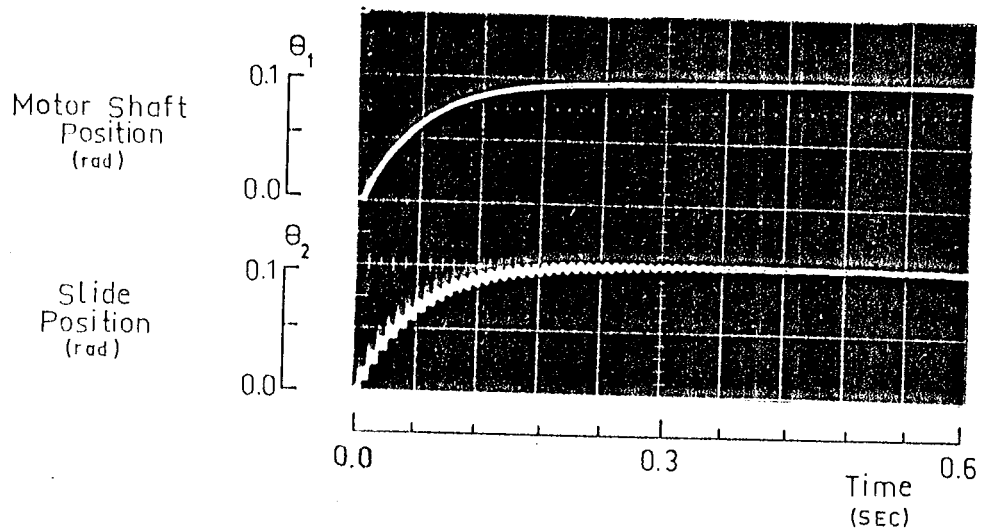


Fig. 5.13 Effect of the Equivalent Slide Inertia ( $J_2^* = 3 J_2$ )

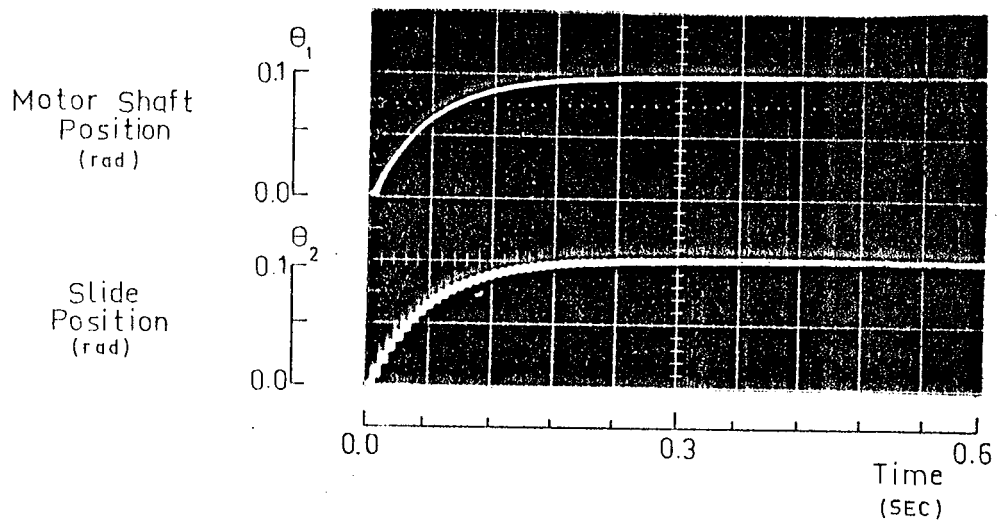


Fig .5.14 Effect of the Equivalent Slide Inertia ( $J_2^* = 2 J_2$ )

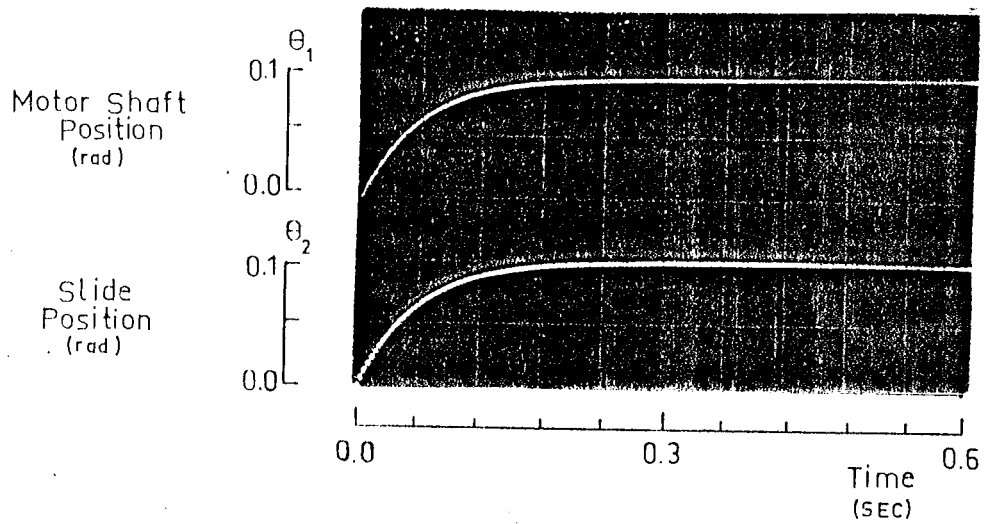


Fig .5.15 Effect of the Equivalent Slide Inertia ( $J_2^* = \frac{1}{2} J_2$ )

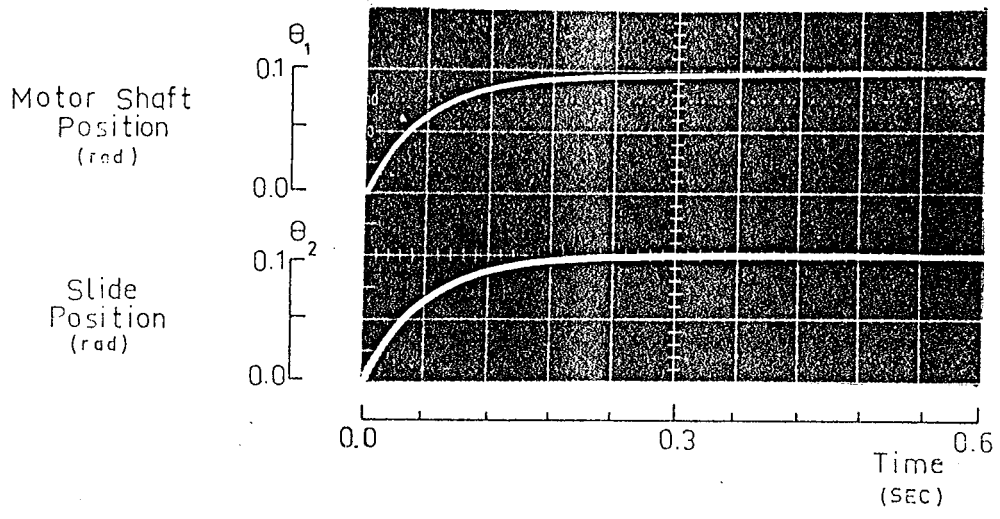


Fig. 5.16 Effect of the Equivalent Slide Inertia ( $J_2^* = \frac{1}{3} J_2$ )

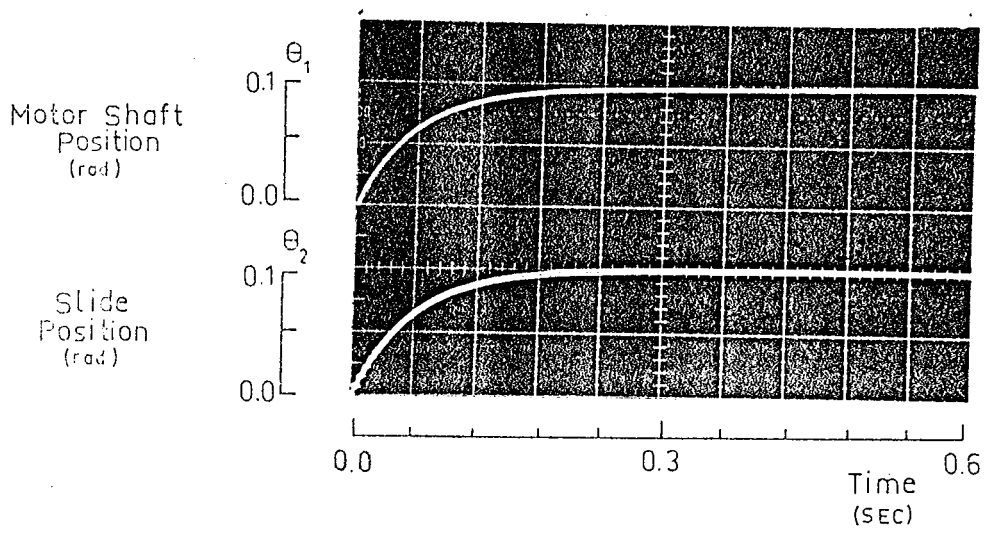


Fig. 5.17 Effect of the Damping ( $D_{tT}^* = 4 D_{tT}$ )

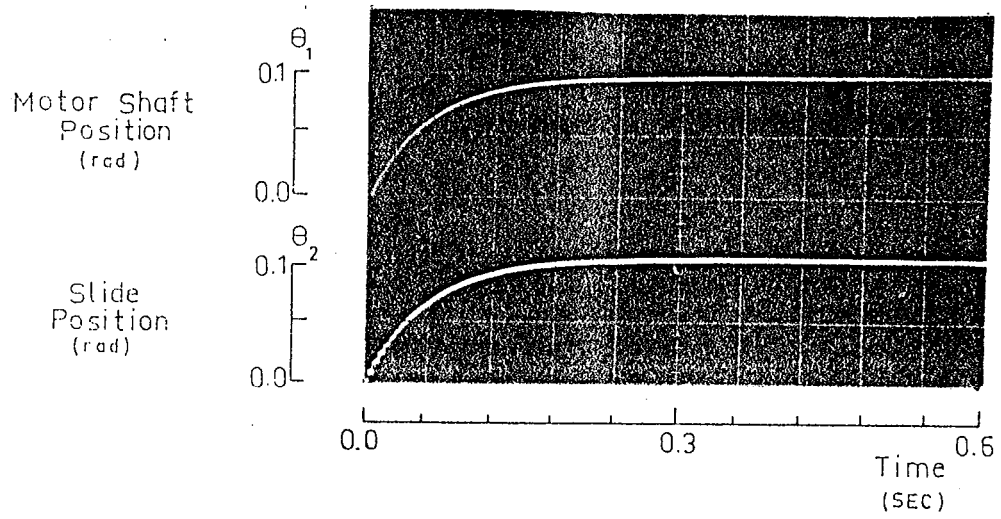


Fig. 5.18 Effect of the Damping ( $D_{tT}^* = 3 D_{tT}$ )

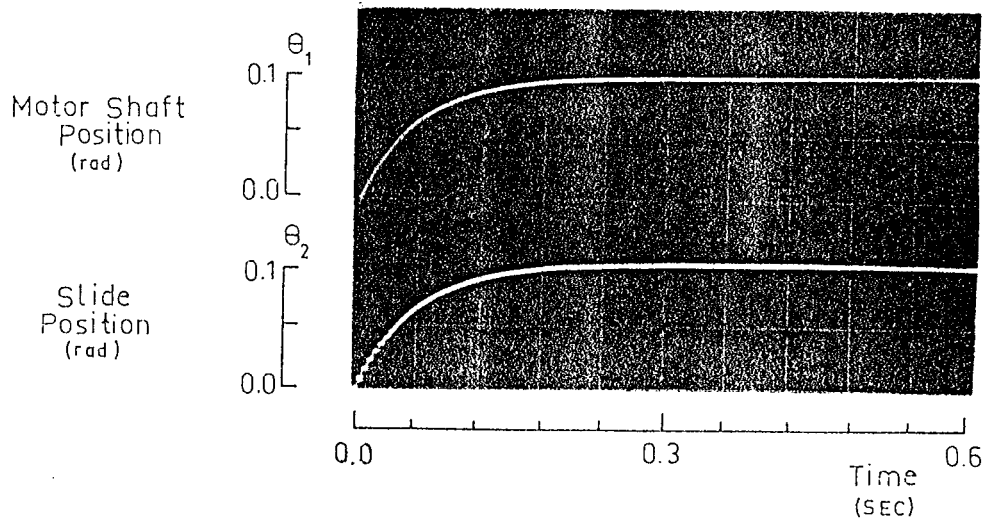


Fig. 5.19 Effect of the Damping ( $D_{tT}^* = 2 D_{tT}$ )

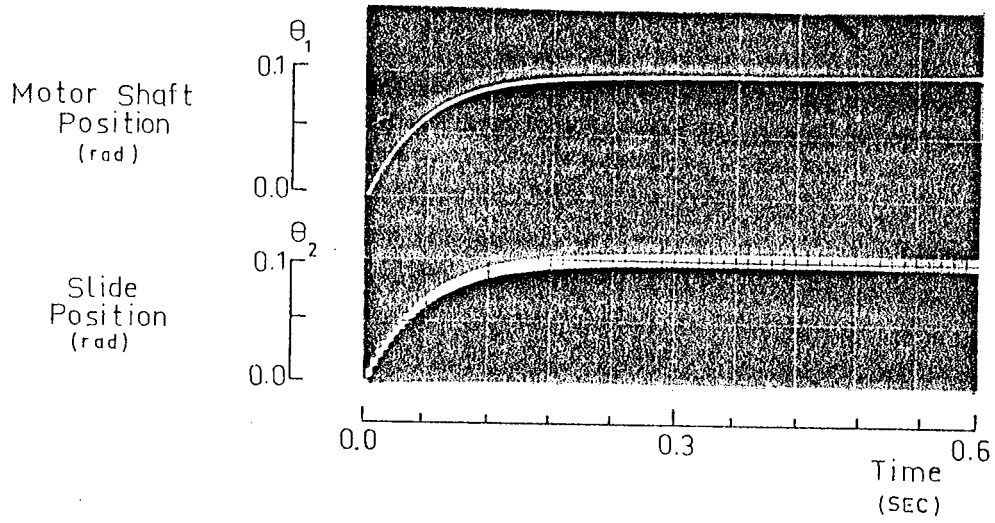


Fig. 5. 20 Effect of the Damping ( $D_{tT}^* = \frac{1}{2} D_{tT}$ )

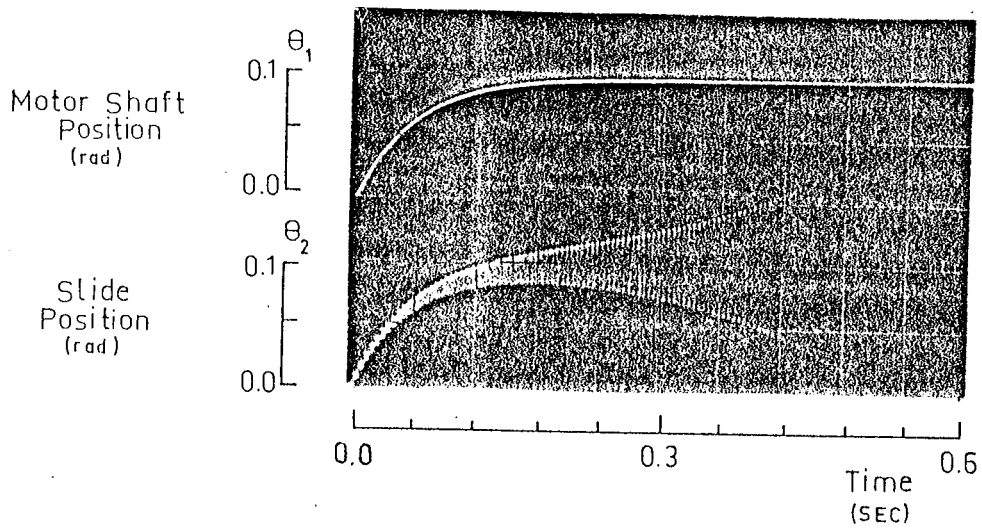


Fig. 5. 21 Effect of the Damping ( $D_{tT}^* = \frac{1}{3} D_{tT}$ )



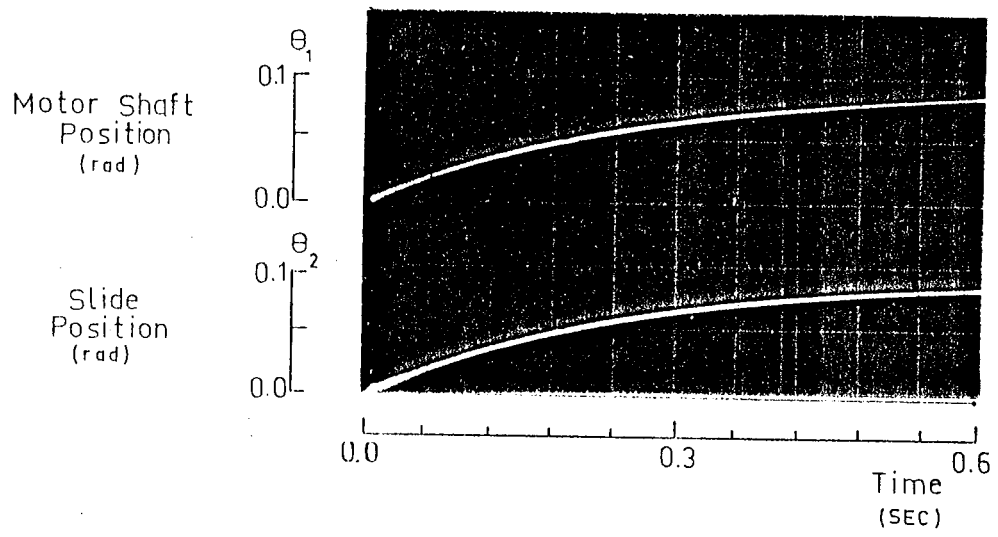


Fig. 5.22 Effect of the Loop Gains ( $K_p^* = \frac{1}{4} K_p$  and  $K_v^* = 4 K_v$ )

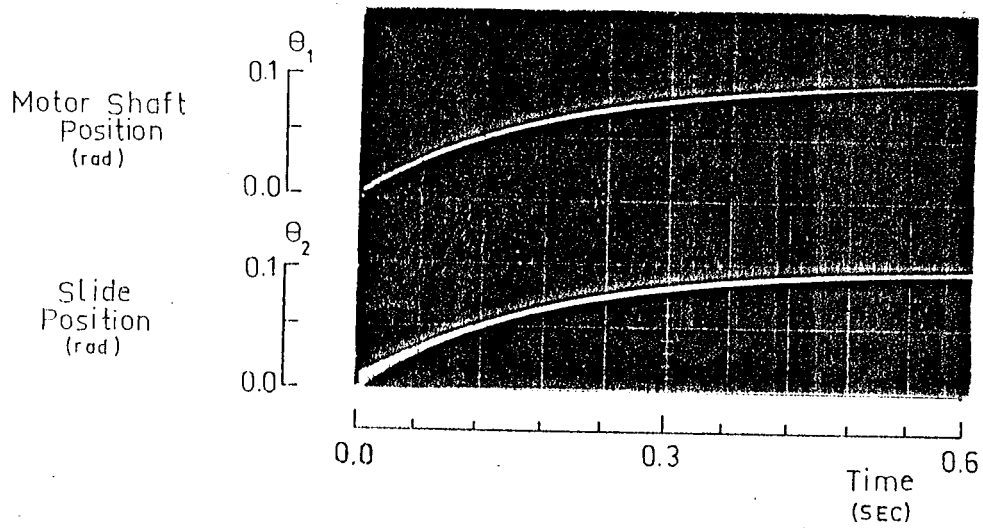


Fig. 5.23 Effect of the Loop Gains ( $K_p^* = \frac{1}{3} K_p$  and  $K_v^* = 3 K_v$ )

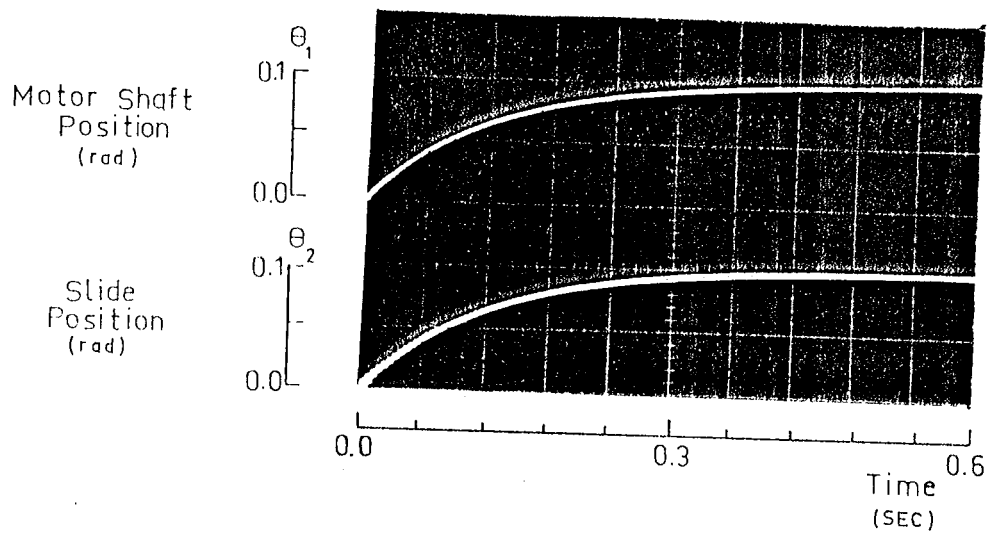


Fig. 5.24 Effect of the Loop Gains ( $K_p^* = \frac{1}{2} K_p$  and  $K_v^* = 2K_v$ )

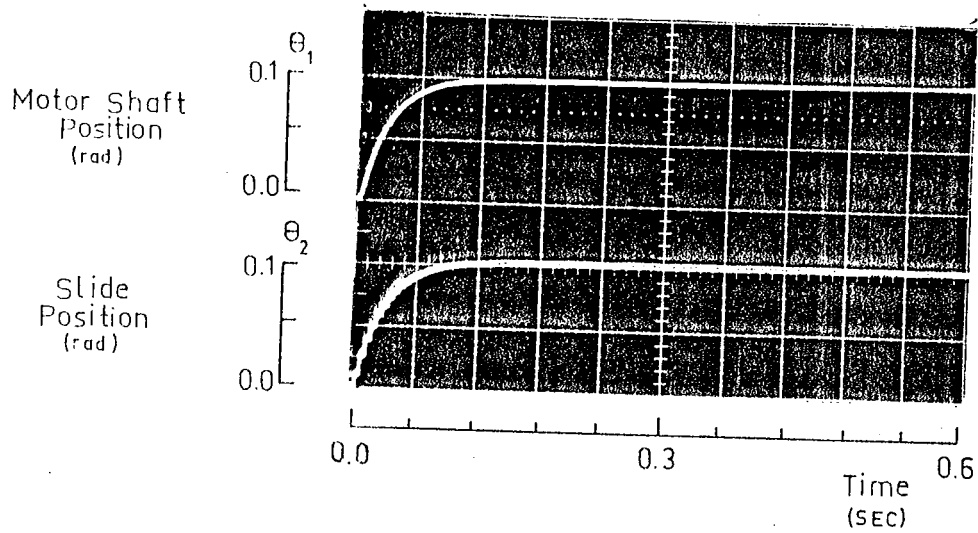


Fig. 5.25 Effect of the Loop Gains ( $K_p^* = 2K_p$  and  $K_v^* = \frac{1}{2} K_v$ )

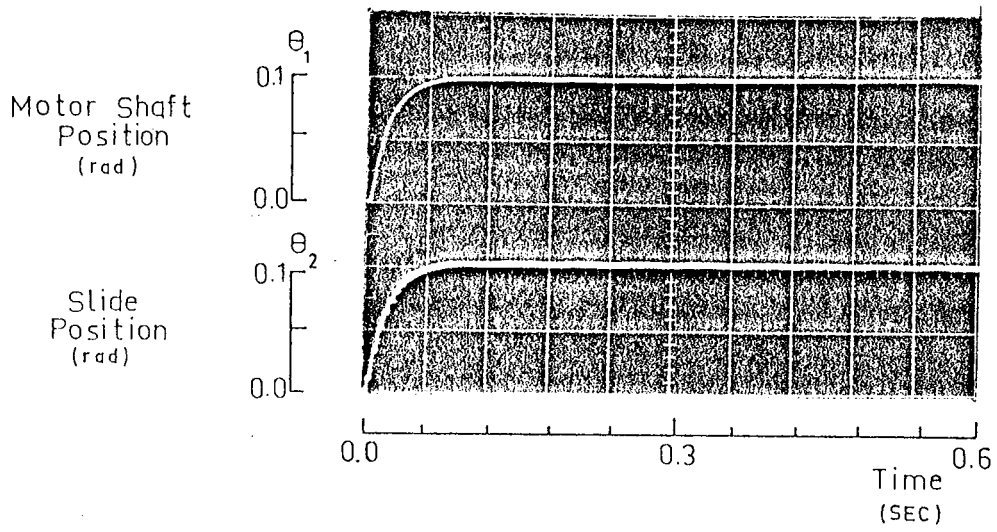


Fig. 5.26 Effect of the Loop Gains ( $K_p^* = 3 K_p$  and  $K_v^* = \frac{1}{3} K_v$ )

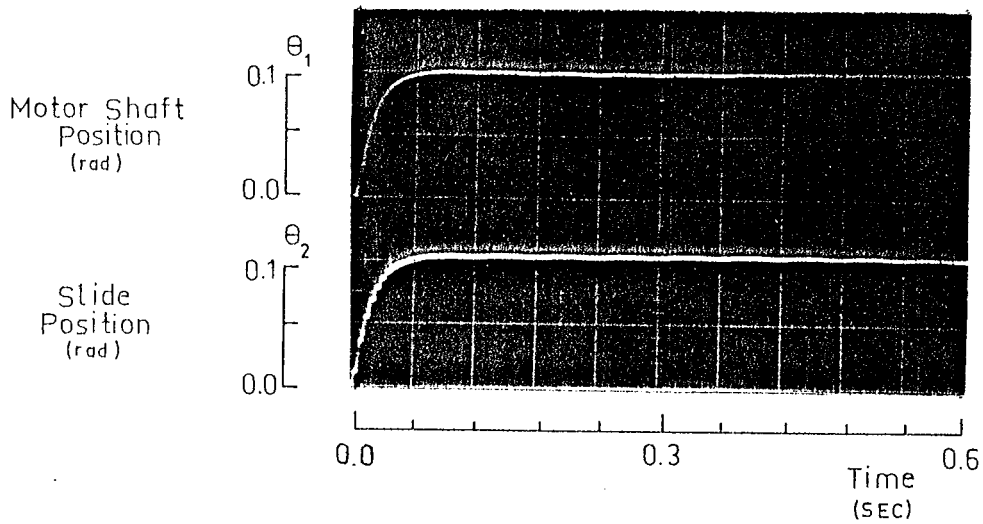


Fig. 5.27 Effect of the Loop Gains ( $K_p^* = 4 K_p$  and  $K_v^* = \frac{1}{4} K_v$ )

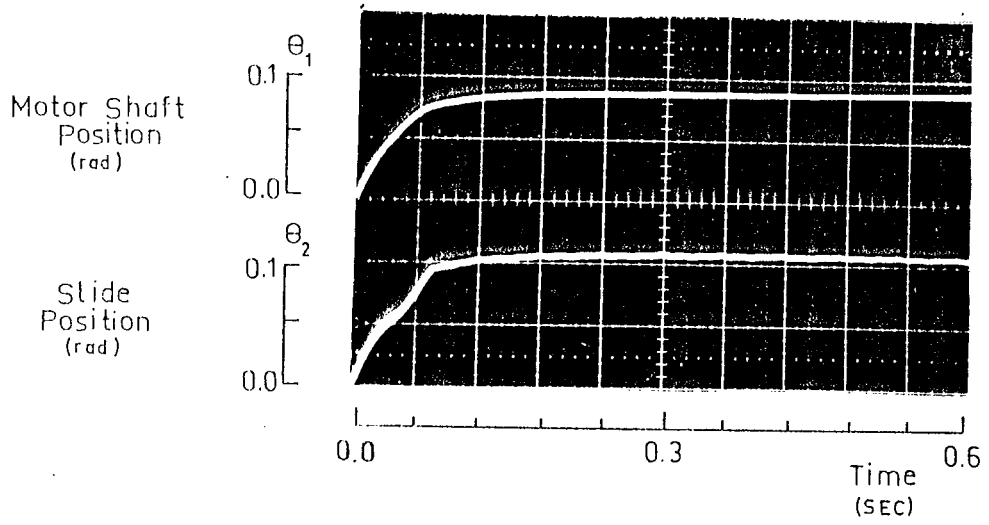


Fig. 5.28 Effect of the Coulomb Friction ( $\mu^* = 3\mu$ )

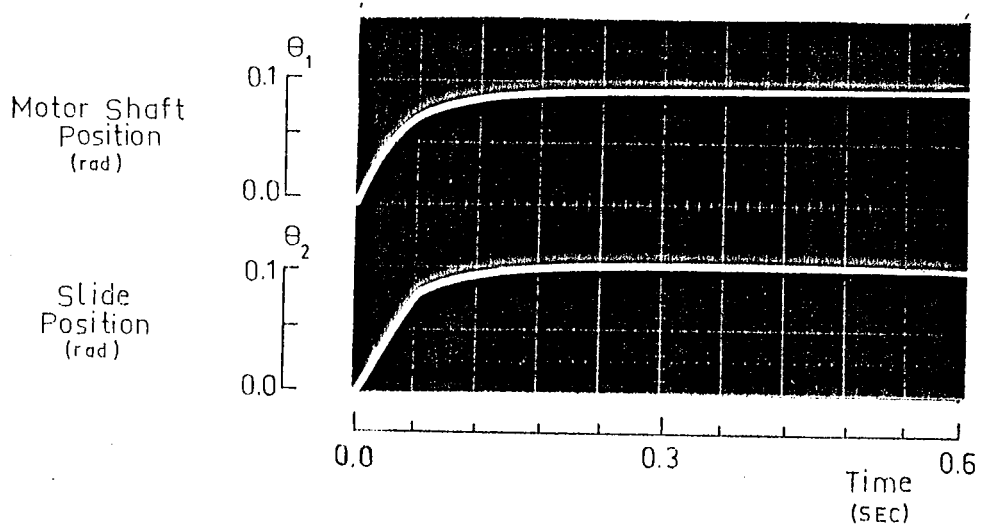


Fig. 5.29 Effect of the Coulomb Friction ( $\mu^* = 2\mu$ )

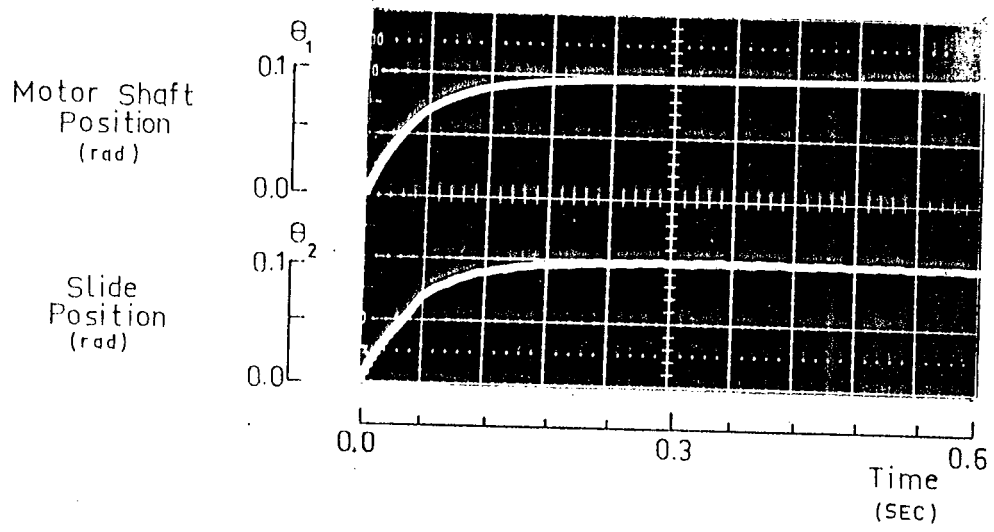


Fig. 5.30 Effect of the Coulomb Friction ( $\mu$ )

## CHAPTER 6

### DISCUSSION AND CONCLUSION

#### 6.1 DISCUSSION

The work reported in the previous chapters has covered the modelling of the feed drive system, basic principles of analog simulation and the application of analog simulation for the evaluation of the dynamic performance of the feed drive systems.

Before drawing the final conclusions from this study, it is preferred to discuss the results presented in the previous chapter. Firstly the similar effects of the parameters on the dynamic performance are to be discussed. These are summarized as follows :

- Increasing the equivalent axial stiffness, has the similar effect as decreasing the damping coefficient of the table.
- Decreasing the equivalent axial stiffness has the similar effect as increasing the equivalent table inertia.
- Decreasing the equivalent table inertia has the similar effect as increasing the damping coefficient.
- Increasing the friction between table and slideway deteriorates the positioning accuracy of the table.
- Increasing position loop gain  $K_p$  , makes the system faster, but increasing velocity loop gain,  $K_v$  , slows down the response.

In machine tools, feed drive systems are required to have high performance. That is the system has to have high acceleration and accurate positioning capabilities. System parameters (size of the components) therefore have to be determined to satisfy these requirements.

As noticed to the responses (figures 5.5 - 5.30) the system response becomes better when :

- a) Stiffness increases up to a certain limit
- b) Inertia decreases
- c) damping increases

If we consider (a) and (b); we see that they are conflicting each other. Equivalent axial stiffness is made up of the stiffness of ball bearing screw, screw - nut connection, bearings and nut - table connection. Increasing equivalent axial stiffness implies an increase in the stiffness of each component. The stiffness of ball screw is proportional to the square of the diameter. To increase the stiffness, diameter has to be increased. But increase in stiffness will result in a larger increase in inertia since it is proportional to the fourth power of diameter. So load on the motor increases. But, in two inertia model, the inertias of the motor, coupling, bearing and ball bearing screw are lumped at motor side and table and tooling are lumped at the other side as a load. Therefore, if the equivalent axial stiffness is increased by way of increasing the diameter of ball bearing screw, the inertia of the motor side increases. This means that the load inertia/motor inertia ratio decreases.

If the equivalent axial stiffness is increased by an increase in screw - nut connection, this can be done either by using different nut or by increasing the amount of preload between nut and the ball screw. Keeping in mind that it will also increase the friction torque which will consequently result in large lost motion and also affect the size of dc motor.

In addition if the torsional equivalent of axial stiffness is increased by way of lead of the ball bearing screw, then equivalent table inertia also increases. An increase in table inertia adversely affects the system performance.

These are the conflicting points and the designer has to find a compromise between them.

The other important point is analog simulation of the system. Analog simulation is an effective way for dynamic analysis but it has some problems about scaling. In this study, because of the characteristic

of modelling, the most big part of inertias is lumped at motor side for two inertia model. Equivalent inertia is much lower than the other inertias (approximately 1/40) as shown in table 5.1. This big ratio creates an important problem on scaling. If five - inertia model are analysed by using analog computer, then very high stiffnesses of ball bearing screw and coupling (approximately  $100 K_{eaT}$ ) cause much more difficulties on time and magnitude scaling. In addition the limited capacity of the analog computer, GP-6, is another point of the difficulties in this study.

## 6.2 CONCLUSION

1- The work of modelling of the feed drive system is more organized to analyse the system.

2- Friction is modelled and included to the model as a non-linear effect.

3- The system equations are adapted to analog computer for simulation. For this purpose, time and magnitude scaling are applied to the equations and analog computer diagrams are prepared.

4- The effects of the system parameters on the dynamic performance are demonstrated by using the analog simulation. The conflictions between parameter variations are explained to help the designer.

5- It is indicated that the two-inertia model is enough for almost of the practical uses.

## 6.3 SUGGESTIONS FOR FUTURE WORK

Evaluation of dynamic performance of feed drive can be developed by considering the following suggestions :

1- A gear box can be used as coupling unit in stead of a coupling.

2- Five inertia model can be used to evaluate the system performance in a large capacity analog computer and results can be compared with two-inertia model.

3- Friction model included the static and kinetic friction can be added to the system model using the analog circuit given in appendix of this model.

4- Backlash can also be added to approach to real system.



#### LIST OF REFERENCES

- 1- Seto, K., Yamada K., 1976. " On the Dynamic Behaviour of Feedback Controlled Feed Drive ", Bulletin of the JSME, Vol.19, No.133, pp.814-821.
- 2- Filiz I.H., 1981. " Computer Aided Design of Feed Drives for N.C. Machine Tools " PhD Thesis, UMIST.
- 3- Ikawa, N., Mizumoto, H., 1975. " A Dynamic Model of Positioning Mechanism of Machine Tool Table ", JJME, pp.157-169.
- 4- Dutcher, J.L. " Servos and Machine Design for Numerical Control ", General Electric Co. Publication GET - 3210.
- 5- Zeleny, J., 1965. " Feed Drives for Numerical Controlled Machine Tools ", Proc 6 th MTDR Conference, pp.391 - 405.
- 6- Thomson, W.T., 1979. " Theory of Vibration with Applications ", Prentice - Hall of India Private Limited, New Delhi.
- 7- Khong, H.P., Bell, R., 1973, " DC Motor Feed Drives for Numerically Controlled Machine Tools ", 14 th Int. MTDR Conference. pp.391 - 405.
- 8- Andreev, G.I. et al, 1977. " DC Motors for Feed Drives on NC Machine Tools ", Machines and Tooling, Vol.48, No.1, pp.15 - 18
- 9- Electro- Craft Corporation, 1977. " DC Motors, Speed Controls, Servo Systems ", An Engineering Handbook, Pergamon Press, New York.
- 10- Steidel, R.F., 1971. " An Introduction to Mechanical Vibrations ", John Wiley and Sons, Inc., New York.
- 11- Jackson, A.S., 1960. " Analog Computation ", McGraw - Hill Book Company.
- 12- Rajaraman, V., 1976. " Analog Computation and Simulation ", Prentice - Hall of India Private Limited, New Delhi.
- 13- Blum J.J., 1972. " Analog Simulation of an AC Automobile generator ", Simulation, Vol.19, No.4 pp.140 - 144.

- 14- Rea, D.P., 1969. " Design of Mechanical Linkages Using an Analogue Computer ", Simulation, Vol. 13, No.1 pp.13 - 23.
- 15- Cuppon, B.C., Bollinger, J.G., 1966. " Simulation of a Machine Tool Drive and Structure on an Analog Computer ", 7 th MTDR Conference pp. 191 - 211
- 16- Shigley, J.E., 1967, " Simulation of Mechanical Systems; an Introduction ", Mc Graw - Hill Book Co., New York.
- 17- Bennett, B.S., 1973. " Parallel Logic Analogue Computation Lecture Notes " Control System Center , UMIST,
- 18- Stephenson, R.E., 1971. " Computer Simulation for Engineers ", Harcourt Brace Jovanovich, Inc, Inc, New York
- 19- Pessen, D.W., 1973. " A Time Scaling Rule for Analog Computers ", Simulation, Vol.20, No.2 pp. 69-71.
- 20- Ashley, J.R., 1970. " Another Approach to Time Scaling the Analog Computer ", Simulation, Vol.15, No.1 pp . 37 - 38.
- 21- Cannon, M.R., 1973. " Magnitude and Time - Scaling of State - Variable Equations for Analog/Hybrid Computation ", Simulation, Vol.21, No.1, PP. 23 - 28.
- 22- Auslander, D.M., 1974. " On Scaling of State - Variable Equations for Analog Computation ", Simulation, Vol.22, No.1, PP. 28 - 29.
- 23- Auslander, D.M., Takahashi, Y., Rabins, M.J., 1974. " Introducing System and Control ", Mc Graw - Hill Book Co., New York.
- 24- Wang, H., Shen, C.N., 1962. " Simulating True Dry Friction on the Analog Computer ", Control Engineering, Vol.9, Pt.2, PP. 91 - 92.
- 25- Parnaby, J., 1968, " Electronic Analogue Computer Study of Non - Linear Effects in a Class of Hydraulic Servomechanisms ", Journal Mechanical Engineering Science, Vol.10, No.4, pp. 346 - 359.

APPENDIX

An analog circuit for a friction model which includes the static and kinetic friction is suggested by Parnaby (25) as follows :

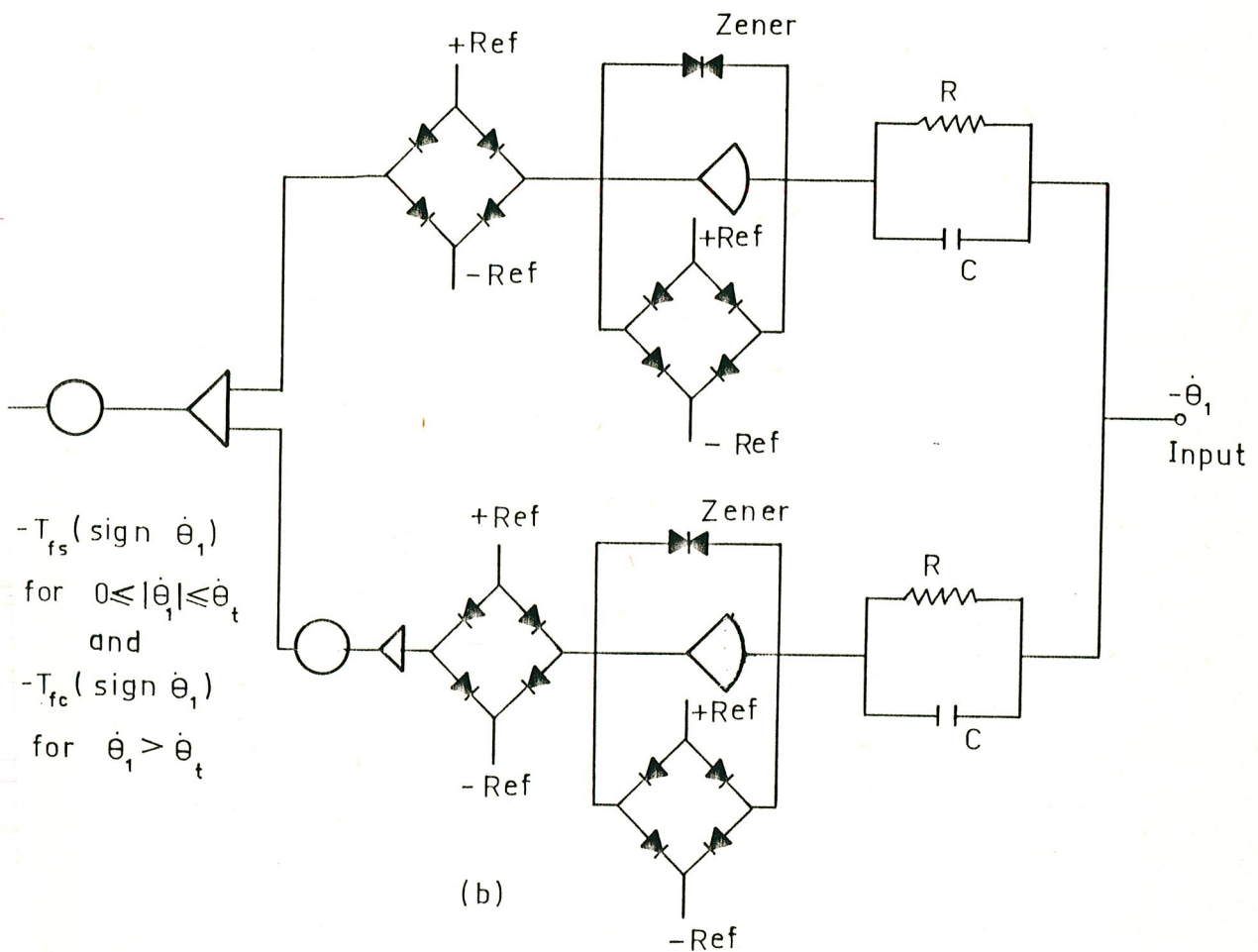
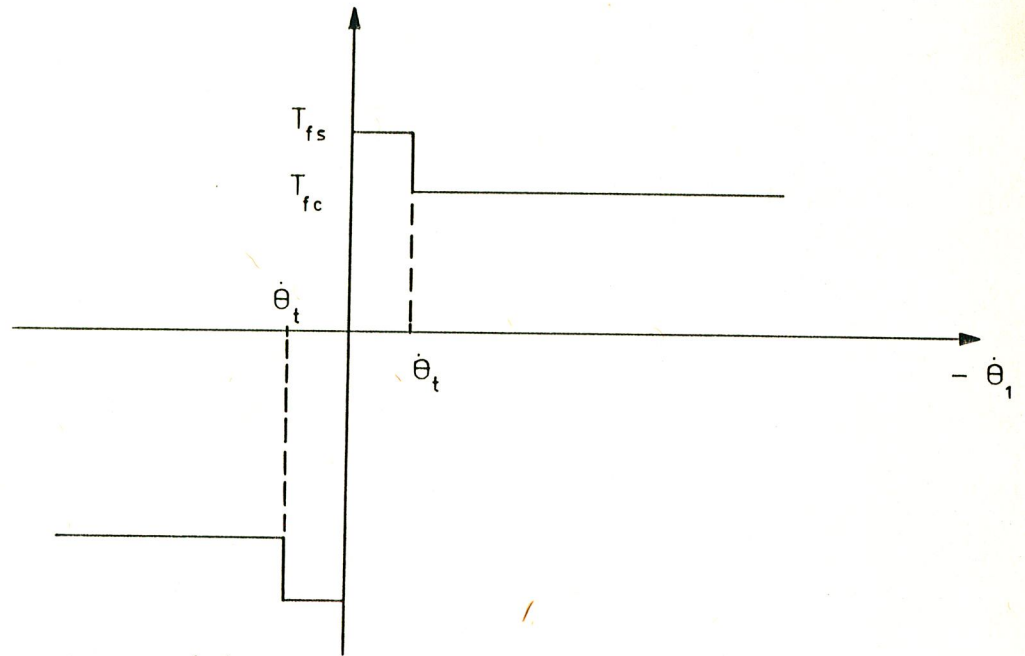


Fig. A A Friction Model and its Analog Circuit